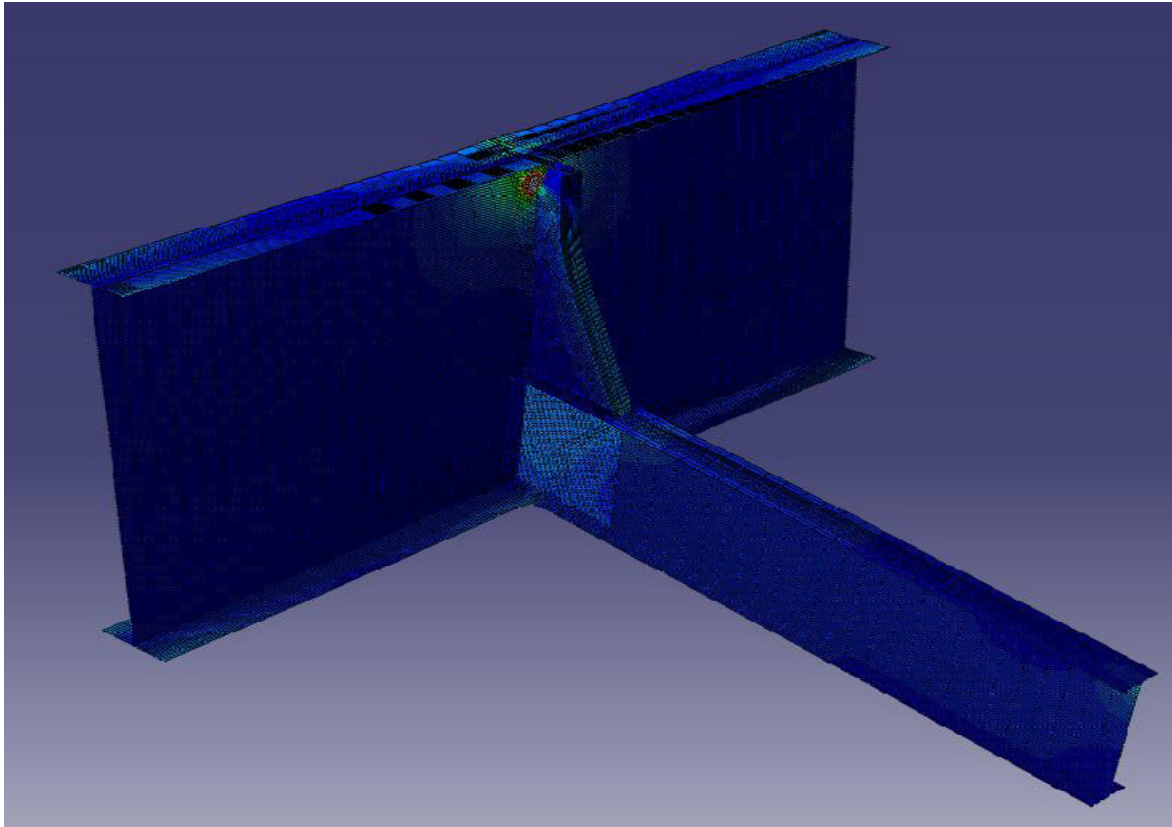


CHALMERS



Analysis of vibration-induced fatigue cracking in steel bridges

Master's Thesis in the Structural Engineering and Building Performance Design

JASIM MOHSIN NASER

FERNANDO SERRANO TOLEDANO

Department of Civil and Environmental Engineering

Division of Structural Engineering

Steel Structures

CHALMERS UNIVERSITY OF TECHNOLOGY

Göteborg, Sweden 2011

Master's Thesis 2010:138

MASTER'S THESIS 2010: 138

Analysis of vibration-induced fatigue cracking in steel bridges

Master's Thesis in the *Structural Engineering and Building Performance Design*

JASIM MOHSIN NASER

FERNANDO SERRANO TOLEDANO

Department of Civil and Environmental Engineering
Division of Structural Engineering
Steel Structures

CHALMERS UNIVERSITY OF TECHNOLOGY

Göteborg, Sweden 2011

Master's Thesis 2010:138

Analysis of vibration-induced fatigue cracking in steel bridges

Master's Thesis in the *Structural Engineering and Building Performance Design*

JASIM MOHSIN NASER

FERNANDO SERRANO TOLEDANO

© JASIM MOHSIN NASER AND FERNANDO SERRANO TOLEDANO, 2011

Examensarbete

Department of Civil and Environmental Engineering

Division of Structural Engineering

Steel Structures

Chalmers University of Technology

SE-412 96 Göteborg

Sweden

Telephone: + 46 (0)31-772 1000

Chalmers Reproservice
Göteborg, Sweden, 2011

Analysis of vibration-induced fatigue cracking in steel bridges

Master's Thesis in the *Structural Engineering and Building Performance design*

JASIM MOHSIN NASER

FERNANDO SERRANO TOLEDANO

Department of Civil and Environmental Engineering

Division of Structural engineering

Steel Structures

Chalmers University of Technology

ABSTRACT

The purpose of this work is to study vibration-induced fatigue cracking in a typical bridge detail, which has shown to be critical according to fatigue. The detail studied is a transversal web stiffener used as floor-beam connection.

Fatigue damage in bridge elements and details is generated by some dynamic effects (vibration, resonance, etc.). The nominal quasi-static load effects in such details are usually relatively low, and thus, a standard fatigue analysis will generally overlook the real load effects in these details.

Fatigue stands for more than 90% of all damage cases reported in steel bridges. Cracking in details can take place in small unstiffened web gaps at which the deformation is concentrated. In many cases, the load effects in such details are magnified (and the number of available loading cycles are decreased) due to dynamic effects. These effects need to be studied in order to avoid this kind of cracking.

FE-model was constructed for the detail where cracks had been observed in the actual bridge. The hot spot method has been used for determining the stresses developed in the detail. By using the trains model HSLM-A producing the dynamic loads on the specific model, it was possible to study the fatigue life for the detail that has the critical response against this kind of loads. Vibration fatigue analysis method is applied and Dirlik method for the response evaluation is adopted.

The modeling was performed using the software ABAQUS.

The work is performed in collaboration between Chalmers and Vectura Consult AB.

Key words:

Fatigue, vibration, frequency domain, hot spot stress, PSD, Dirlik, HSLM

Analys av vibrationsinducerade utmattningssprickor i stålbro

Master's Thesis in the *Structural Engineering and Building Performance design*

JASIM MOHSIN NASER

FERNANDO SERRANO TOLEDANO

Institutionen för Bygg- och miljöteknik

Avdelningen för Konstruktionsteknik

Stålbyggnad

Chalmers tekniska högskola

SAMMANFATTNING

Syftet med detta arbete är att studera vibrationer som orsakas av utmattningssprickor i en specifik bro detalj, vilka har visat sig ha en avgörande roll när det gäller utmattning. Den detalj som studerats är en livavstyvare som används i anslutningen mellan huvud och tvärbalk i en järnvägsbro av stål.

Utmattningsskador i brons delar och detaljer har genererats av vissa dynamiska effekter (vibrationer, resonans, etc.). Den nominella kvasistatiska belastningseffekten i sådana detaljer är vanligtvis relativt liten, och därmed skulle en standardanalys av utmattningen bortse från den verkliga lastens effekter i dessa detaljer.

Utmattning står för mer än 90% av alla skadefall som rapporterats i stålbroar. Sprickbildning uppkommer från spänningskoncentrationer, vilka kan uppkomma av deformation i balkliv deformationen koncentrerats. I många fall är lasteffekterna i sådana detaljer förstörade (och antalet tillgängliga lastcykler är minskade) på grund av dynamiska effekter. Dessa effekter behöver studeras för att undvika denna typ av sprickbildning.

En FE -modell gjordes för att analysera detaljen där sprickor konstaterats i bron. "hot spot"-metoden har använts för att bestämma spänningen i detaljen. Genom att använda tåglastmodell HSLM-A för att ta fram de dynamiska lasterna i modellen var det möjligt att studera utmattning i balklivet för de detaljer som har en kritisk utsatthet för denna lasttyp. Vibrationsutmattningsanalys tillämpades och Dirlik-metoden för responsen i Täthetsfunktionen användes.

Modelleringen utfördes med hjälp av programvaran ABAQUS.

Arbetet har utförts i samarbete mellan Chalmers och Vectura konsult AB.

Nyckelord:

Utmattning, vibration, frekvensspann, hot spot spänning, PSD, Dirlik, HSLM

Contents

ABSTRACT	V
NYCKELORD: UTMATTNING, VIBRATION, FREKVENSSPANN, HOT SPOT SPÄNNING, PSD, DIRLIK, HSLM	VI
CONTENTS	VII
PREFACE	X
NOTATIONS	XI
1 INTRODUCTION	1
1.1 Problem description	1
1.2 Aim of studies	1
1.3 Limitations	1
1.4 Methodology	1
2 FATIGUE	3
2.1 Background	3
2.2 Fatigue phenomenon	3
2.3 Fatigue analysis	5
2.3.1 S-N curves	5
2.3.2 Stress cycle's history	6
2.3.3 Stress histogram	6
2.4 Fatigue assessment by Palmgren-Miner method	7
2.5 Fatigue assessment of welded structures	9
2.6 Nominal stress method	9
2.7 The hot spot method	10
2.7.1 Assessment of hot spot stress	11
2.7.2 Hot spot method in Finite Element Modeling	13
2.7.3 Evaluation of fatigue using hot spot stress	13
2.7.4 Hot spot S-N design curves	13
3 SIGNAL PROCESSING	15
3.1 Time and frequency domain	15
3.2 The Fourier transform	17
3.2.1 The Nyquist sampling theorem	18
3.2.2 Spectral leakage and windowing function	19
3.3 Power Spectral Density PSD	20
3.3.1 Characterization of time process using statistical measures	21
3.3.2 Characterization of frequency process using statistical measures	22

4	LOAD MODEL	24
4.1	Moving point load traversing a simply supported beam	24
4.2	The train load	26
4.3	Relation between geometric dimensions, load speed and Fourier components	28
4.4	Load in frequency domain	30
4.4.1	Averaged load spectrum	32
4.4.2	Peak-hold load spectrum	33
4.4.3	White noise load spectrum	33
5	THE SDOF SYSTEM	34
6	VIBRATION FATIGUE	37
6.1	Fatigue life estimation	37
6.2	Probability density function PDF	37
6.2.1	Narrow Band solution	38
6.2.2	Dirlik empirical solution	38
7	FE MODELING	42
7.1	FE modeling of the detail from the bridge	42
7.2	Structural response of the detail	45
7.2.1	Natural frequencies and mode shapes	45
7.2.2	Frequency response analysis	48
8	RESULTS	48
8.1	Response evaluation	51
8.1.1	Output PSD from the averaged load	51
8.1.2	Output PSD from peak-hold load	53
8.1.3	Output PSD from the white noise load	54
8.2	Fatigue analysis	54
8.2.1	Fatigue estimation from the averaged load	55
8.2.2	Fatigue estimation from the peak-hold loading	57
8.2.3	Fatigue estimation from the white noise loading	58
8.2.4	Comparison of fatigue life between averaged, peak-hold and white noise loads	58
9	CONCLUSIONS	60
10	FURTHER STUDIES	60
11	REFERENCES	62
A.	APPENDIX A	65

B. APPENDIX B	67
C. APPENDIX C	72

Preface

In this Master's Thesis, the work has been done to determine whether it is efficient to study the fatigue life for the constructional details using frequency domain analysis instead of time domain processing. The dynamic effects created by the moving load on a structure can amplify the static loads and thus have to be taken in consideration.

This work could not be done without people that gave a great hand. We would like to express our sincerest gratitude to our supervisors Johan Jonsson and Tobias Larsson from Vectura Consulting AB for their great help and support.

Words of gratitude should be said to our examiner Professor Mohammad Al- Emrani at Chalmers University of Technology for his help and coordinating.

We would also like to thank our opponents Anders Carlsson and Mónica Lucas Romero for their support and feedback.

Unlimited thank and appreciation words for our families. Thank you for supporting and believing in us. Without you we could have done nothing.

Göteborg, March 2011

Jasim Mohsin Naser

Fernando Serrano Toledano

Notations

Roman upper case letters

A	Area [m ²]
C	Damping
C_r	Critical damping
$D(r)$	Dynamic amplification factor
DOF	Degree Of Freedom
E [0]	Number of upward zero crossings in a signal
E [P]	Number of peaks in a signal
F	force [N]
FFT	Fast Fourier Transform
IFT	Inverse Fourier Transform
FRF	Frequency Response Function
G	Acceleration
Hz	Frequency
I	Moment of inertia [m ⁴]
HSLM	High Speed Load Model
IIW	International Institute of Welding
K	Stiffness matrix
L	Length[m]
M	Mass matrix
MDOF	Multi Degree Of Freedom
N_i	Cycles to failure at constant stress range
N_C	Number of cycles (2 millions) at which the reference value of the fatigue strength is defined
N_D	Number of cycles(5 Millions) at which the constant amplitude fatigue limit is defined
N_L	Number of cycles(100 millions) at which the cut-off limit is defined
N	Number of samples in a signal
P	Load [N]
PSD	Power Spectral Density
RMS	Root Mean Square
SDOF	Single Degree Of Freedom
T	Time [s]
U	Displacement matrix
U	Amplitude of the forced response
U_0	Static displacement
Z	The distance from the centre of mass [m]

Roman lower case letters

a	Acceleration
c	Speed (m/s)
c_r	Critical speed (m/s)
dS	The stripes width under the pdf curves
f^n	Frequency number Hz
f_S	Spring force [N]
f_D	Damping force [N]
f_t	Applied force [N]
f_N	Nyquist frequency
f_s	Sampling frequency
f_c	Highest frequency contained in the signal
h	Time interval in a signal
i	Imaginary number
k	Stiffness [N/m]
k	S-N curve constant
x	Displacement [m]
m	Mass [Kg]
m_n	Moment from the PSD where n can be 0,1,2 and 4
\mathcal{M}	Moment [KN m]
n_i	Number of cycles
pdf	Probability density function
$p(S)$	Stress probability
r	Frequency ratio
rms	Root mean square
s	Root to the equation of motion for a SDOF system
t	Thickness [m]
t	Time[s]
v	Speed [m/s]
w	Thickness of the parent element [m]
u	Displacement
\dot{u}	Velocity vector
\ddot{u}	Acceleration vector
$u_p(t)$	Trail solution of displacement
$\dot{u}_p(t)$	Trail solution of velocity vector
$\ddot{u}_p(t)$	Trail solution of acceleration vector

Greek letters

$\Delta\sigma$	Nominal stress range (nominal stress)
$\Delta\sigma_C$	Reference value of the fatigue strength at 2 millions cycles
$\Delta\sigma_D$	Constant amplitude fatigue limit
$\Delta\sigma_L$	Cut-off limit
$\Delta\sigma_{equ}$	Equivalent stress range
$\Delta\tau_C$	the shear stress range that cause failure after 2 millions cycles
$\Delta\tau_D$	the shear stress range that cause failure after 100 millions cycles
σ_{ln}	Linear distribution of the stresses in the weld toe
σ_m	Membrane stress
σ_b	Bending stress
σ_{nlp}	Non linear distribution of the stresses in the weld toe
$\sigma_{0.4t}$	Stress at 0.4t distance from the weld toe
$\sigma_{0.1t}$	Stress at 1.0t distance from the weld toe
$\sigma_{0.9t}$	Stress at 0.9t distance from the weld toe
$\sigma_{1.4t}$	Stress at 1.4t distance from the weld toe
σ_{hs}	Hot spot stress
$\sigma_{geo,act}$	Geometric stress for a the detail in question
$\sigma_{geo,ref}$	Geometric stress for a reference detail
γ	Irregularity factor
γ_{Ff}	Partial safety factor for fatigue load
γ_{Mf}	Partial safety factor for fatigue strength
ξ	Damping factor
δ_f	Frequency resolution
φ	Damping
$\alpha(f)$	The harmonic response
f_n	Resonance frequency [Hz]
ζ	Damping factor
ω_n	Undamped natural frequency
ω_d	Damped natural frequency
Ω	Frequency
$\alpha(\Omega)$	Transfer function
α_c	Speed parameter

1 Introduction

1.1 Problem description

Fatigue life evaluation of civil engineering structures is usually based on cyclic load considering only static effects. By adopting this approach for dynamically loaded structures it might not capture the whole picture. When the load subjected on the structure excite it with frequencies close to the structure's resonance limit, additional fatigue damage can arise.

Fatigue estimation for structures containing a dynamic behavior, need to be considered by a dynamic approach. Fatigue can be analyzed by the traditional time domain method, through the Palmgren-Miner damage calculation. However, this presents a practical problem when the time history is too long.

In this thesis both methodologies to perform fatigue analysis will be presented.

1.2 Aim of studies

This master thesis aims to study the hot spot methodology to estimate fatigue damage in structures that withstand dynamic loading in areas with stress linearity. Furthermore, the study aims to demonstrate the usability of using the frequency domain of a structure to evaluate fatigue.

1.3 Limitations

The limitations of this thesis are:

- The train is regarded as a set of point loads moving along the bridge.
- Speeds of the trains are slow.
- Vehicle-bridge interaction and track imperfection are not considered.
- In order to examine the validity of the frequency domain approach a main-beam cross-girder connection is investigated by Finite Element Modeling.
- The stiffness of welds is not taken into consideration.
- No measurements are performed to evaluate the validity of the FE-model.

1.4 Methodology

The work develops numerous methodologies and steps to carry out the task systematically. First, a literature survey from papers, books and earlier theses on the topic have been studied. This gave a good foundation to start the thesis.

Then, a load has been created to simulate the trains. This load is considered as a random load, so in order to analyze it, it has to be transformed into the frequency domain. This is done by the help of the Matlab software.

Afterwards, a FEM Software program-ABAQUS is used to analyze the problem. A specific detail of the bridge over Söderström is modeled and simulated in ABAQUS. First, a modal analysis is performed to analyze the structural response of the structure. Then, random load is applied to obtain the stresses that cause fatigue failure. In order to obtain these stresses, the hot spot method is applied in a critical part of the model where there were cracks in the original detail from the bridge.

To reach to a reasonable conclusion, a fatigue damage caused by these stresses is calculated by adopting vibration fatigue methodology and by using the Dirlik formula. Some comparisons between different load spectrums are performed. This has been made to examine the validity of each of these loads and to study the usability of vibration induced fatigue methodology.

2 Fatigue

2.1 Background

Fatigue is the most common cause of failure in steel structures. “Fatigue is not a new phenomenon, it has puzzled researcher for over 200 years. The problem with fatigue attracted attention with the use of metal in structures. One of the first to investigate the fatigue phenomenon was Wöhler 1819-1914. He conducted systematic investigations on train axles and why they broke during repeated loads lower than the static design load. Tests from fatigue investigations were plotted in diagrams with the stress range on the vertical axis and the number of cycles on the horizontal axis. To get a better overview of the results, the diagram was log scaled. A linearly result of the components fatigue life was thereby possible to detect. The diagrams developed to a standard for predicting fatigue life of details and structures, still used today and known as Wöhler diagrams or S-N diagrams, where S stands for the stress range and N for the number of cycles.

Fatigue failures occur in details or whole structures due to repeated loading, the load levels leading to a fatigue failure are lower than the static resistance. The most important factor concerning fatigue is the stress range $\Delta\sigma$, but the exact form of the stress range has a marginal influence. Generally fatigue only develops through tension stresses; hence compressive loading will not contribute to fatigue. The definition is only valid if the material is free from residual stresses, which seldom is the case due to processes such as rolling and welding. This makes it possible for compressive loading to contribute to fatigue”, Larsson [33].

Despite two hundred years of studies and investigations in the area of fatigue, it is not totally clear yet. In addition, it is the most common reason for failure in metallic structures. These extensive efforts haven’t identify the mechanism of fatigue, thus fatigue is empirically investigated even if analytical methods are used for the practical treatment of fatigue problems [23].

2.2 Fatigue phenomenon

Fatigue occurs when the material is exposed to a repeated stress cycles varying over time. Thus it is a process of time; it starts with slip formation that grows until it reaches a critical size that will cause fracture in the material. Slip formation is enhanced by the stress concentration due to internal defects or external hole in a plate as a notch.

When a load is applied in cyclic form, this fluctuation will open up and close micro cracks. As the load cycles increase, the crack length will increase for each application of the load. When the crack reaches its critical length, fracture will occur.

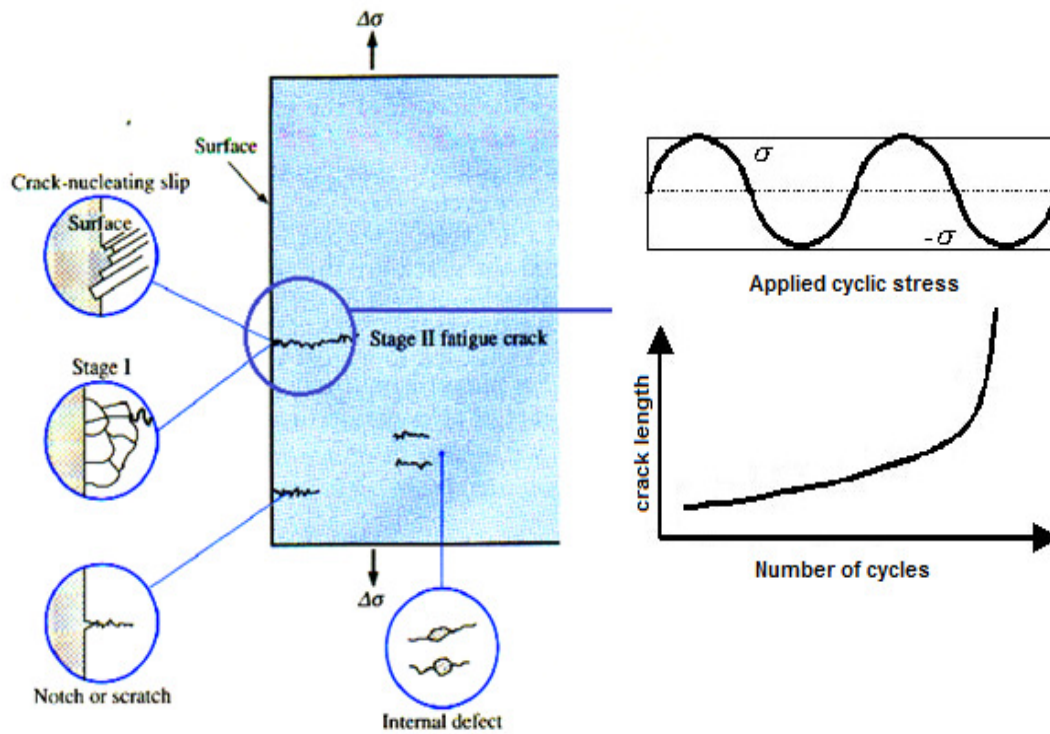


Figure (2-1) Fatigue in materials [4]

The process of fatigue consists of three main stages:

Stage 1: Crack initiation

Stage 2: propagation of one dominant crack

Stage 3: Final fracture

The first stage is crack initiation: The material in the structure suffers micro slips, these slips grow along slip planes due to shear stress driven process. The crack initiation is usually extended over a few grains leading to micro cracks in the neighboring grains resulting in one or few dominating cracks. The slip that is made by the shear is not homogenously distributed through the material. A single cycle can cause a microscopic intrusion into the material which can form a micro crack. The mechanism that arises in the first cycle will be repeated in the cycles after and cause the crack to extend in each cycle [24].

The second stage in the fatigue process is when the stress field that governs the cracks cause a further growth and form a dominant crack with a perpendicular path to the tensile stress axis. If the stresses are influencing the growth of the crack then the final stage, fracture, will be reached.

2.3 Fatigue analysis

If a structure has to be design to withstand fatigue loading or determining the remaining life expectancy it is often done by using Wöhler curves. In the following chapter the fatigue design process is explained using Wöhler curves, determination of stress levels from load history, how to calculate accumulated fatigue damage and the usability of hot spot method.

2.3.1 S-N curves

When evaluating fatigue, most design codes employs the concept of Wöhler or S-N curves, however the shapes of the curves or detail categories as they also are called can differ between codes.

In the European code EN 1993-1-9 [4] the fatigue life of details is evaluated by using 14 detail categories, defined as the stress range a detail can endure during 2×10^6 cycles, see notation (1) in Figure (2-2).

Notation (2) in Figure (2-2) indicates the constant amplitude limit. For a detail only affected by a constant stress range, the design of the predicted fatigue life can follow the horizontal design curve. A constant cyclic loading is quite rare in structural engineering. The constant amplitude fatigue limit starts after $N = 5 \times 10^6$ cycles. If the stress range instead is varying the curve with the inclination $m = 5$ should be used.

The cut of limit corresponds to $N = 1 \times 10^8$ cycles, notation (3) in Figure (2-2). A varying stress range below this limit does not contribute to accumulated fatigue damage. Stresses that do exceed the cut of limit contribute to a damage accumulation.

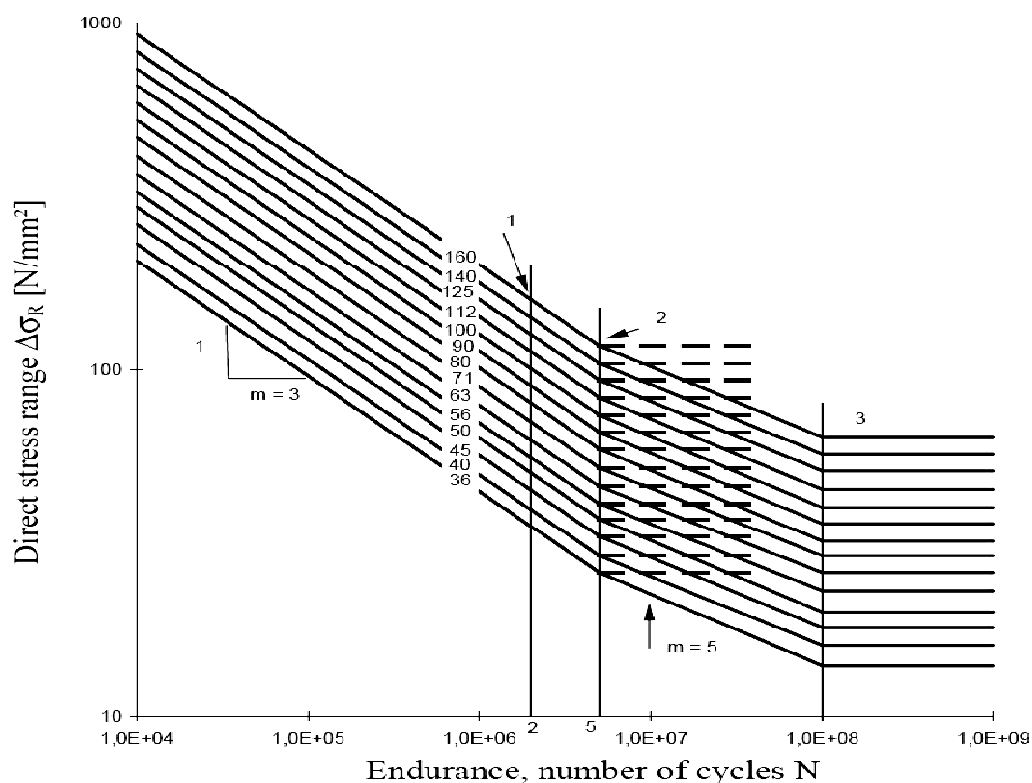


Figure (2-2) Fatigue strength curves for normal stress ranges [1]

2.3.2 Stress cycle's history

In order to determine the loading a structure has endured, its stress history has to be established. Stress histories can either consist of constant or variable load amplitudes. In case of constant cycles they can be evaluated directly. Variable amplitude stresses cannot be evaluated directly due to its arbitrary load amplitude. See Figure (2-3) as an example of variable stress amplitude.

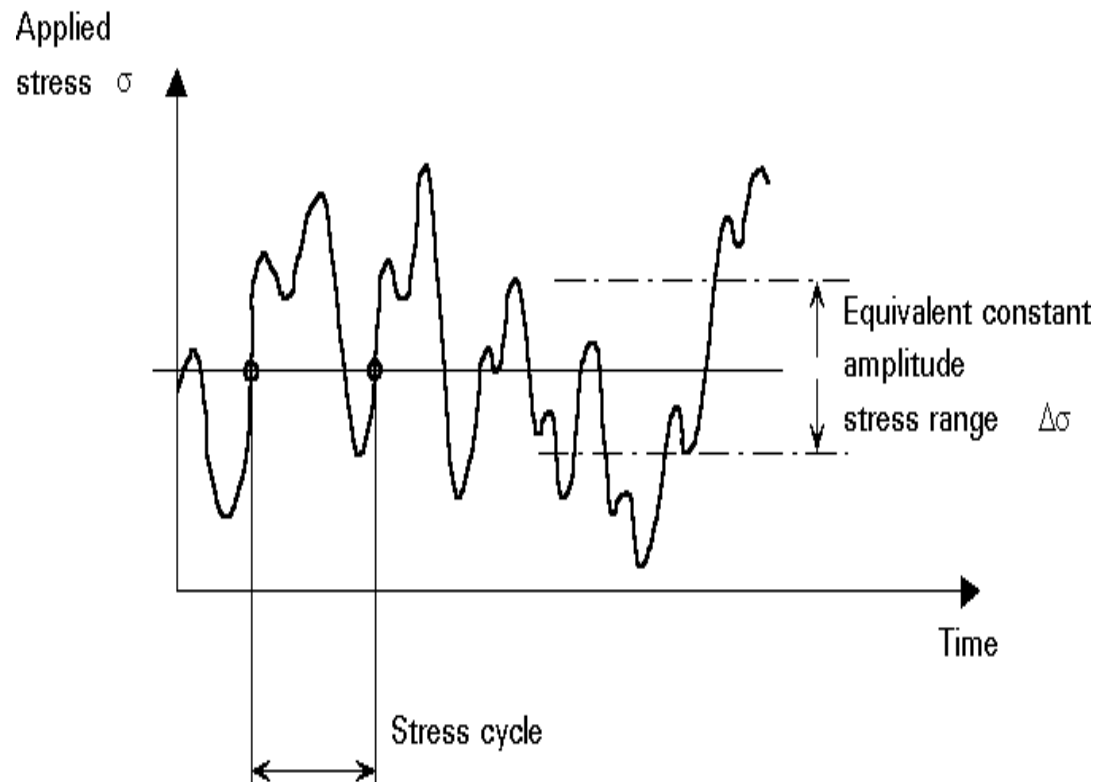


Figure (2-3) Variable amplitude stress history [2]

The two most common methods to evaluate the number of load cycles and stresses a detail has been exposed to are, the 'reservoir' counting method and the rainflow method, The final fatigue estimation however is nearly the same using these methods.

2.3.3 Stress histogram

The variable stress cycles is converted into stress histogram by summing up the stress range of equal amplitude in order to determine the number of load cycles for each stress range [4]. Where the stress histogram (or stress spectrum) consist of a number of constant stress range blocks. Each block is categorized by its number of cycles n_i and its stress range $\Delta\sigma_i$ [1]. Figure (2-4) shows the stress histogram or stress range distribution.

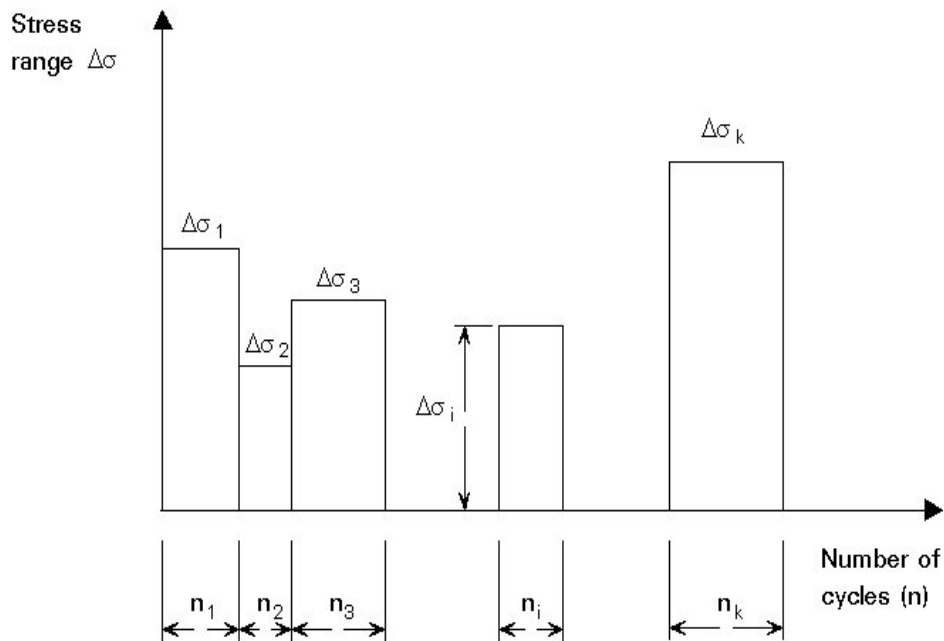


Figure (2-4) Stress histogram or stress range distribution [1]

2.4 Fatigue assessment by Palmgren-Miner method

The remaining fatigue life of a structure can be determined by the Palmgren–Miner method, it assumes a linear summation of the damage in a detail. The summation of the cycles at each stress range is divided by the available cycles to failure, see equation (2-1).

$$D = \sum_{i=1}^k \frac{n_i}{N_i} \quad (2 - 1)$$

Where

D Cumulated damage

n_i Cycles of stress range

N_i Cycles of stress range $\Delta\sigma_i$ to cause failure

The stresses that are causing fatigue can either be normal stresses or shear stresses. Depending on the structural detail analysed, the values of the limits $\Delta\sigma_D$, $\Delta\sigma_L$ and $\Delta\tau_L$ are obtained according to the following relations [4].

$$\Delta\sigma_D = \left(\frac{2}{5}\right)^{1/3} \Delta\sigma_C \quad (2-2)$$

$$\Delta\sigma_L = \left(\frac{5}{100}\right)^{1/5} \Delta\sigma_D \quad (2-3)$$

$$\Delta\tau_D = \left(\frac{2}{100}\right)^{1/5} \Delta\tau_C \quad (2-4)$$

where

$\Delta\sigma_C$	Stress range that causes failure after 2×10^6 cycles
$\Delta\sigma_D$	Stress range that causes failure after 5×10^6 cycles
$\Delta\sigma_L$	Stress range that causes failure after 100×10^6 cycles
$\Delta\tau_C$	Shear stress range that causes failure after 2×10^6 cycles
$\Delta\tau_D$	Shear stress range that causes failure after 100×10^6 cycles

The stress limits as stated above are essential to identify which equation to be used in order to obtain the number of cycles to failure. The equations are as follows:

If

$$\gamma_{Ff} \cdot \Delta\sigma_i \leq \frac{\Delta\sigma_D}{\gamma_{Mf}} \quad (2-5)$$

Then

$$N_i = 2 \cdot 10^6 \left[\frac{\Delta\sigma_C / \gamma_{Mf}}{\gamma_{Ff} \cdot \Delta\sigma_i} \right]^3 \quad (2-6)$$

But when

$$\frac{\Delta\sigma_D}{\gamma_{Mf}} > \gamma_{Ff} \cdot \Delta\sigma_i \geq \frac{\Delta\sigma_L}{\gamma_{Mf}} \quad (2-7)$$

Then

$$N_i = 5 \cdot 10^6 \left[\frac{\Delta\sigma_D / \gamma_{Mf}}{\gamma_{Ff} \cdot \Delta\sigma_i} \right]^5 \quad (2-8)$$

And only when

$$\gamma_{Ff} \cdot \Delta\sigma_i \leq \frac{\Delta\sigma_L}{\gamma_{Mf}} \quad (2 - 9)$$

Then

$$N_i = \infty \quad (2 - 10)$$

Where, γ_{Ff} represents the partial safety factor that covers the uncertainties in estimating the load parameters and the design life of the structure. γ_{Mf} is representing the partial safety factor that covers the uncertainties of the detail parameters. $\Delta\sigma_i$ represents the stress range.

2.5 Fatigue assessment of welded structures

Fatigue is most common to take place in areas where there is a stress concentration. Welding areas can be considered as stress concentration points. One important factor that affects the fatigue strength in welded structures is the direction of the weld.

The strength of the weld is controlled by the weld profile and its quality control. Eurocode 1993-1-9 classifies structural details into many categories arranged in tables according to the type of detail, the stress direction, the mode of cracking, manufacturing, tolerance and weld types.

2.6 Nominal stress method

Nominal stress method is the most used fatigue design method. The nominal stress σ_{nom} is defined as the global stress in the cross section according to Navier's equation (2-11).

$$\sigma_{nom} = \frac{F}{A} + \frac{M}{I} * Z \quad (2 - 11)$$

Where

F	Force [N]
A	Area [m ²]
M	Moment [kNm]
I	Moment of inertia [m ⁴]
Z	Distance to the bending edge [m]

Equation (2-11) is taking into consideration the relation between the applied load and the bending moment.

Eurocode3 [4] defines 14 fatigue resistance S-N curves for nominal stresses. In the case of multiaxial fatigue where there are normal and shear stresses at the same area then the damage of the both stresses will be summed up. Eurocode 1993-1-9 [4] recommends the total damage ratio to be less than or equal to one, as Equation (2-12) specify.

Where D_σ represent the normal stress damage ratio while D_τ represents the shear stress damage ratio.

2.7 The hot spot method

The hot spot stress is defined as the maximum extrapolated stress range at the weld toe. The hot spot stress method is applicable to complicated stress conditions due to structural discontinuity or complicated geometry. Welded joints can be considered as hot spot areas where the principle stresses work perpendicularly to the weld toe.

The hot spot stress method is applicable for the following situations [6].

- Where there is no clear definition for the nominal stress, as a result of complex geometric effects.
- In joints that cannot be compared with a classified joint configuration in the relevant design code.
- If the parallel or the angular misalignment between plates involved is greater than normal, thereby preventing use of the nominal stress method.

Hot spot stress is simply the range of the stresses that can be created in the hot spot areas due to notch effects. Notch stresses can be obtained by summing up the membrane stress σ_m , bending stress σ_b and the non-linear stress σ_{nlp} where membrane stress represents the mean stress all the way through the plate thickness. The bending stress is obtained by using the stress curve through the plate thickness by drawing a straight line through the point where the membrane stresses meet the plate's centre line. The non-linear stresses represent the stresses that are generated at the notch because of the non-linearity in the stress flow. Figure (2-5) shows the non-linear stress distribution across the plate thickness.

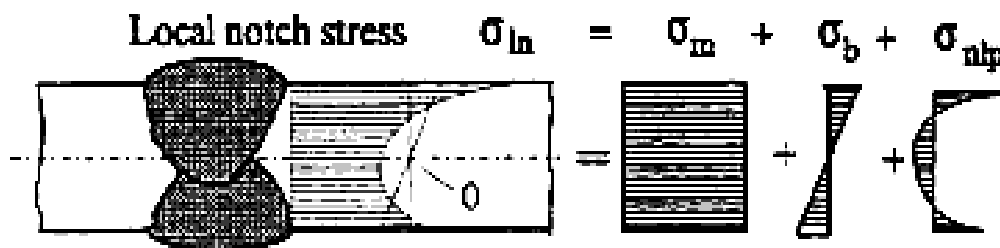


Figure (2-5) Non-Linear stress distribution across the plate thickness [5]

The methodology of the hot spot stresses is all about excluding the non linear stresses from the notch stresses because it is hard to estimate what the toe weld geometry will look like when designing the detail.

The purpose of determining hot spot stresses is to determine the stresses next to weld toe. The Hot spot method depends on the weld characterization and the direction of the weld and its location. Examples where it can be used are (a), (b) and (c). See Figure (2-6).

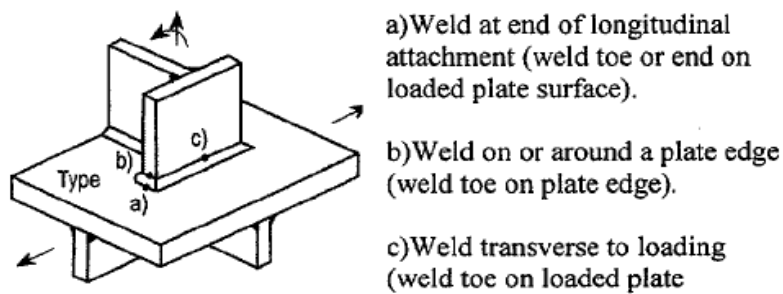


Figure (2-6) Types of hot spots in welded structures [5]

2.7.1 Assessment of hot spot stress

The hot spot stress is a geometric stress for a structural detail. In order to evaluate this detail, it is important to observe the areas where non-linear stress distribution is taking place. The toe of the weld is one of these areas.

In order to obtain the hot spot stress, strain gages can be used. IIW recommend a distance of $0.4t$ and $1.0t$ from the weld toe to place strain gages. The extrapolation is defined in such way that the effects of the global geometry of the weld (flat, concave, convex) and the condition at the weld toe (angle, undercut) are not included in the geometric stress. Figure (2-7) indicates to where the strain gages have to be installed.

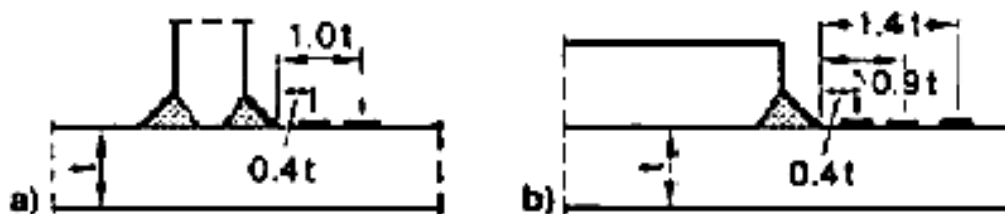


Figure (2-7) Strain gage positioning for the hot spot stress determination [7]

(a) Transverse stiffeners. (b) Cover plate ends.

Equation (2-13) is used to calculate the hot spot stress from the linear extrapolation of stress values at the assigned points [5], where σ_{hs} represents the hot spot stress.

$$\sigma_{hs} = 1.67 \sigma_{0.4t} - 0.67 \sigma_{1.0t} \quad (2 - 13)$$

Figure (2-8) shows the extrapolated nominal stress in a welded joint.

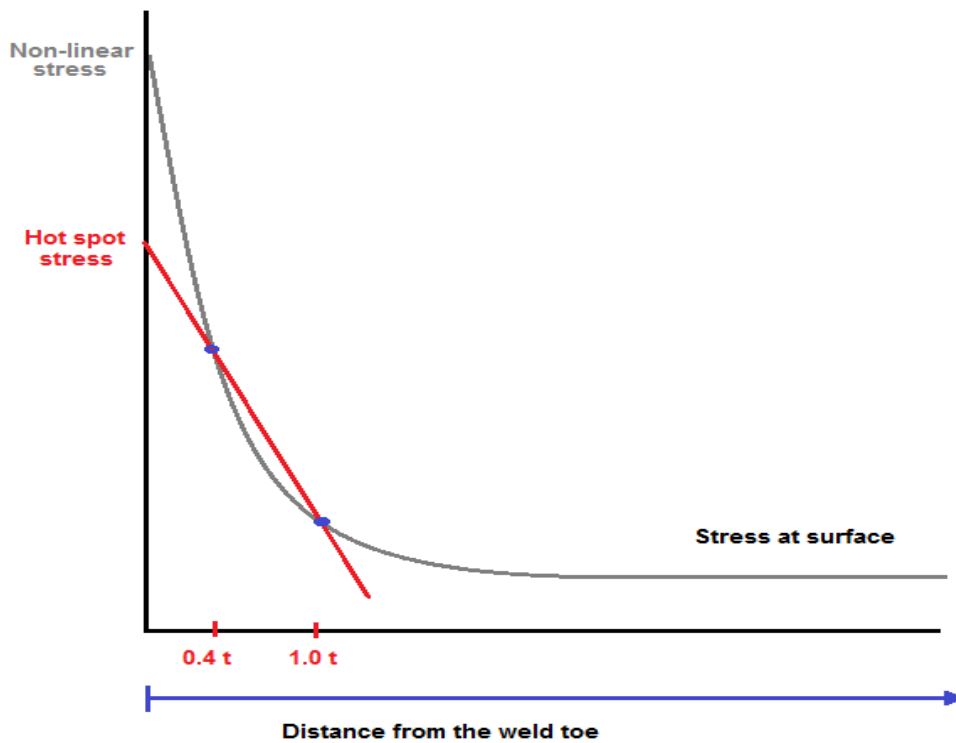


Figure (2-8) Stress distribution in welded joint

In case there is an area of stiff elastic supports i.e. a web or a stiffener, another quadratic relation is to be used. Here the extrapolation points have to be placed at '0.4t', '0.9t' and '1.4t' from the toe of the weld, see equation (2-14).

$$\sigma_{hs} = 2.52 \cdot \sigma_{0.4t} - 2.24 \cdot \sigma_{0.9t} + 0.72 \cdot \sigma_{1.4t} \quad (2 - 14)$$

2.7.2 Hot spot method in Finite Element Modeling

According to Niemi & Marquis [5], the accuracy in determining hot spot stress analytically and by using FEM is in the range of $\pm 10\%$.

The requirements of the International Institute of Welding (IIW) to use hot spot method in Finite Element Modeling are [6]:

- The ratio between the largest and smallest dimensions of an element must not exceed 3.
- The element types which allow a linear stress distribution through the thickness of the plate should be chosen; Eight-node shell elements or 20-nodes solid elements are recommended.
- When shell elements adopted, they should be placed at the neutral axis of the plate and the stiffness of the weld should be considered, for example by modeling the weld using tilted shell elements.
- First element size adjacent to the weld toe and with a perpendicular direction to the weld should be accurately taken in order to get correct results. The distance between the weld toe and the element centre or the nearest integration point should not be greater than '0.4t'.
- The transition to a fine element mesh must be gradual.
- The FE model must be able to explain the stress variation along the weld toe.

2.7.3 Evaluation of fatigue using hot spot stress

It is recommended that the stress component perpendicular to the length of the weld is used to calculate the hot spot stress. It is also important to check the magnitude of the stress component parallel to the weld [5].

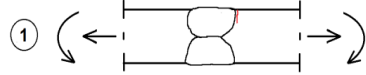

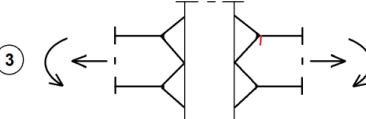
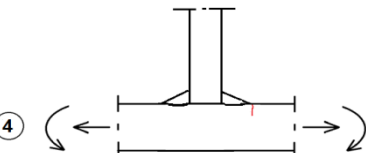
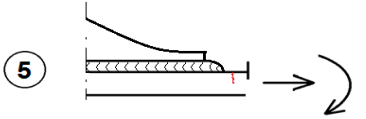
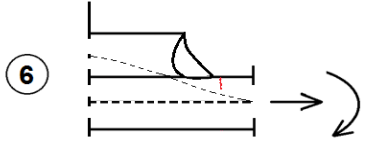
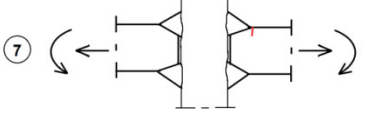
Using the hot spot method to evaluate fatigue has some limitations [6]:

- 1- The stress determined using the hot spot stress approach must be perpendicular to the weld, so for the other types of stresses which are the parallel stresses and shear stress have to be determined using the nominal stress method.
- 2- Hot spot stress methods is only suitable for cracks at the toe of the fillet and butt welds. For the other type of cracks, this method is no longer applicable.
- 3- The method imposes more requirements on the density of the FE mesh.
- 4- The angular or the parallel misalignment in the joint should be considered as well.

2.7.4 Hot spot S-N design curves

The fatigue strength S-N curves for the hot spot stress are similar to the nominal stress S-N curves. There are 7 types of details that have been recommended by Eurocode [4] and IIW.

Table [2-1] Detail categories for use with geometric (hot spot) stress method

Detail category	Constructional detail	Description	Requirements
112		1) Full penetration butt joint	1) - All welds ground flush to plate surface parallel to direction of the arrow. - Weld run-on and run-off pieces to be used and subsequently removed, plate edges to be ground flush in direction of stress. - Welded from both sides, checked by NDT. - For misalignment see NOTE1
100		2) Full penetration butt joints	2) - Welds not ground flush. - Weld run-on and run-off pieces to be used and subsequently removed, plate edges to be ground flush in direction of stress. - Welded from both sides. - For misalignment see NOTE1
100		3) Cruciform joint with full penetration K-butt welds.	3) - Weld toe angle $\leq 60^\circ$. - For misalignment see NOTE1
100		4) Non load-carrying fillet welds.	4) - Weld toe angle $\leq 60^\circ$. - See also NOTE 2.
100		5) Bracket ends. Ends of longitudinal stiffeners.	5) - Weld toe angle $\leq 60^\circ$. - See also NOTE 2.
100		6) Cover plate ends are similar joints.	6) - Weld toe angle $\leq 60^\circ$. - See also NOTE 2.
90		7) Cruciform joint with load carrying fillet welds.	7) - Weld toe angle $\leq 60^\circ$. - For misalignment see NOTE1 - See also NOTE 2.

NOTE1 This table does not cover effects of misalignment; they have to be considered explicitly in determination of stress.

NOTE2 This table does not cover fatigue initiation from the root followed by propagation through the throat.

3 Signal Processing

In structural engineering there are many interesting signals that affect the structures, therefore it is important to be measured and analyzed. These signals are typically the deflections, applied loads, stresses or many other relevant physical magnitudes of a structural element.

Signal Processing is used to analyze and extract information from signals. A signal is defined as any physical quantity that varies with one or more independent variables such as time. In the reality, most of signals are continuous-time. However, to be processed by a computer, a continuous-time signal has to be first sampled in time into a discrete-time signal [29].

The Fourier transforms are often used to transform a problem from one domain to another domain where it is much easier to solve or analyze. The two domains of a Fourier transform have physical meaning and are called the time domain and the frequency domain.

Signals can be divided into two groups, those that have a fixed behavior and those that change randomly. Deterministic signals are fixed and can be determined by a mathematical expression. However, Future values in random signals cannot be predicted. To analyze its behavior it is necessary to use probability and statistics [29].

This study analyzes a deterministic signal that simulates a random process. Furthermore in many applications, deterministic signals are described via statistical models as random signals.

3.1 Time and frequency domain

When the signal changes with a constant amplitude through the time, it will shapes a regular sinusoidal signals that can be seen in Figure (3-1) (a) while in Figure (3-1) (b) the signal is changing in amplitude and frequency.

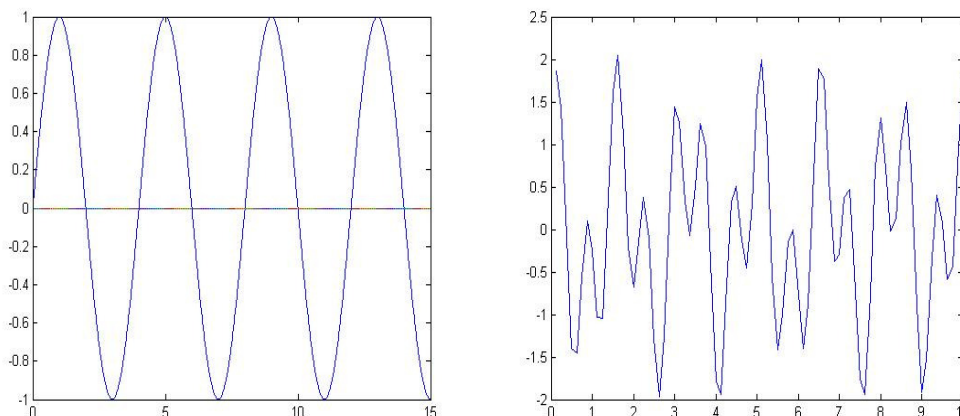


Figure (3-1) Time domain: (a) Sinusoidal vibration with constant amplitude. (b) Random vibration.

It is easy to predict the next cycle for the constant vibration where the signal is in the case of regular sinusoidal signals but this kind of signals rarely happen in reality. In the other hand, when the next cycle cannot be predicted due to the change of amplitude with time, the process is called random since it can only be described statistically.

Fourier analysis decomposes any random signal into a set of sine wave functions with different amplitude, frequency and phase, including square waves and triangle waves. This representation is called deterministic because the individual sine waves can be determined at every time point. This process is still represented in the time domain [9].

However, as an extension of Fourier analysis, Fourier transform allows any engineering signal to be presented as a function of frequency. Hence, this defines the amplitude of harmonics in a periodic wave. In fact, this is called the frequency spectrum of the wave, which inform about the frequency content. Frequency domain is another way of representing a signal.

Signals are convenient to analyze in the frequency domain. Moreover, many signals and systems are specified by their frequency characteristics.

Engineering processes can produce many different types of signals and Figure (3-2) helps to characterize these types of processes in the time and frequency domains. In Figure (3-2) (a) a narrow band process is shown which is built of sine waves that covers a narrow range of frequencies, while in (b) the broad band process is covering a wide range of frequencies. These types of processes are difficult to be distinguished in the time domain but not in the frequency domain.

Figure (3-2) (c) shows a perfect sine wave signal which can only be decomposed into one frequency component. On the other hand, a white noise process (d) is made up of sine waves covering the whole frequency range.

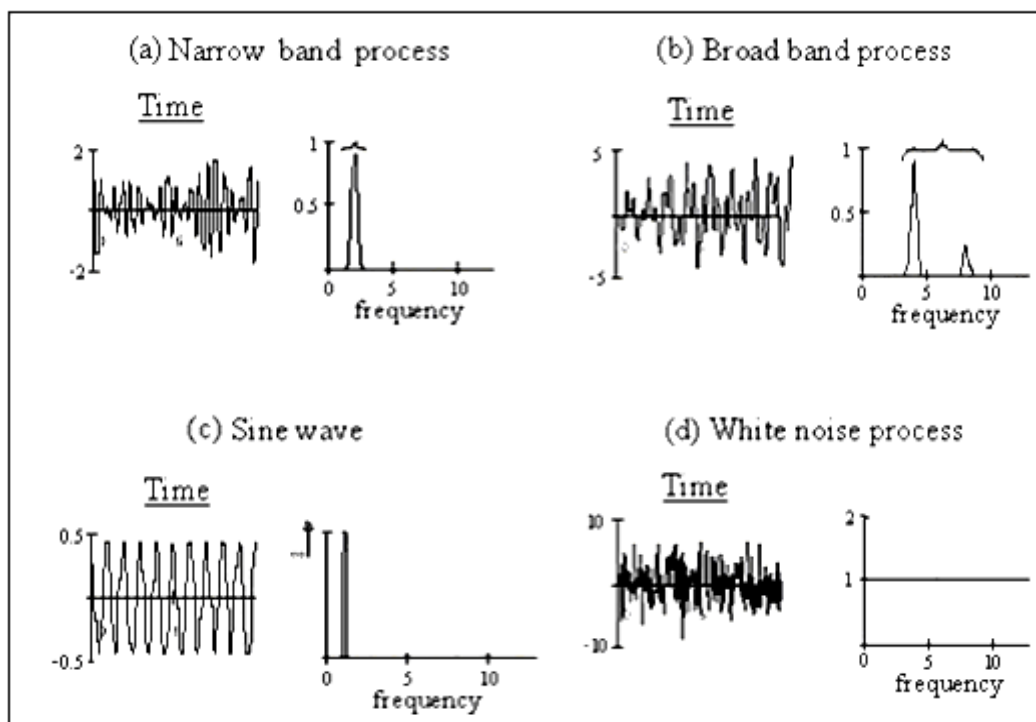


Figure (3-2) Equivalent time histories and Fourier spectrums [9]

3.2 The Fourier transform

The Fourier transform is an operation that transforms a complex function of a real variable into another. In signal processing, this operation is used to transform the domain of the original function from the time to the frequency domain representation. This new domain describes which frequencies are present in the original function.

Fourier analysis demonstrates that any periodic function can be expressed as the summation of number of sinusoidal waves of varying frequencies by amplitude and phase [9]. This function works as decomposing the wave into many waves in each point who have the same frequency with randomly changing amplitude and then summing up the amplitudes using algebra [11].

The Discrete Fourier Transform (DFT) is a specific kind of Fourier transform used in Fourier analysis. But the DFT requires an input function that is discrete. Such inputs are created by sampling a continuous function. However, the DFT can be computed efficiently in practice using a Fast Fourier Transform (FFT) algorithm [31].

Fast Fourier Transform is a fast method for calculating Discrete Fourier Transform, which indeed is a discrete version of continuous Fourier transform. Consequently, historically continuous form of the transform was discovered, then discrete form was created for sampled functions and afterwards an algorithm for fast calculations of discrete version was formed. Figure (3-3) shows the mechanism of the Fast Fourier Transform and the Inverse Fourier Transform.

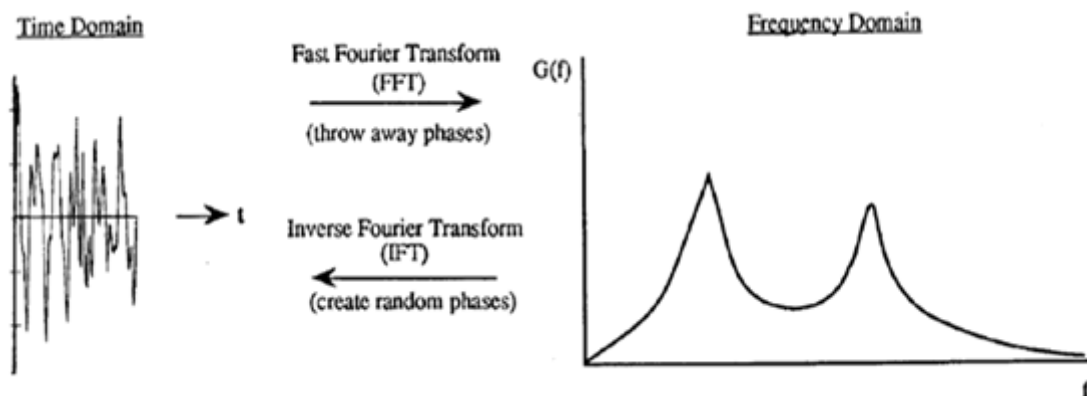


Figure (3-3) Time domain and frequency domain – Source [13]

DFT is a mathematical function while FFT is a number of algorithms to compute a DFT. The most common FFT is the Cooley-Tukey algorithm. This is a divide and conquer algorithm that recursively breaks down a DFT of size $N=N_1 N_2$ into many smaller DFTs of sizes N_1 and N_2 . In addition, as it is said before, an FFT is a faster way to obtain the same result: in order to compute a DFT of N points, it takes (N^2) operations, while an FFT takes only $(N \log N)$ operations [31].

In order to maximize the speed of the FFT, the length of the input data should be to the power of 2 [9]. In the case of the input length is not to the power of 2 it is a good idea to extend the size to the next higher power of 2 and pad additional space with zeros.

The Fast Fourier Transform (FFT) outputs a complex number given with respect to frequency. A sine wave of amplitude (A), frequency (f) and phase (j) is represented in the frequency domain by a peak at (f). If the magnitude of the FFT function is plotted, the area under the peak is the amplitude of the sine wave. However, if the argument of the FFT is plotted, the area under the curve is the initial phase [9].

All the information of the signal is retained in both time and frequency domain. Nevertheless, if only the magnitude of the different sine wave is of interest, the frequency domain representation can be done in terms of power spectral density as it will be explained later.

3.2.1 The Nyquist sampling theorem

The Nyquist sampling theorem provides a recommendation for the sampling interval required to avoid aliasing. Aliasing appears when a signal is discretely sampled at a rate that is insufficient to capture the changes in the signal.

It may be stated basically as follows: “*The sampling frequency should be at least twice the highest frequency contained in the signal.*” [32]

Or in mathematical terms:

$$f_s = 2 f_c \quad (3 - 1)$$

Where f_s is the sampling frequency, and f_c is the highest frequency contained in the signal.

One requirement for the FFT algorithm is that the number of samples of the signal has to be equal to the power of 2.

$$N = 2^n \quad (3 - 2)$$

Then, if the signal is sampled at time intervals h , the sampled length is basically Nh . According to the Nyquist theorem, the highest frequency component of a sampled signal that can be identified without aliasing is the Nyquist frequency [29].

$$f_N = \frac{f_s}{2} = \frac{1}{2h} \quad (3 - 3)$$

The FFT algorithm gives the amplitudes of the sine waves of the signal over the frequency bandwidth from 0 to f_N . In order to apply the Fourier analysis, the signal must be treated as periodic, with a period equal to the sample length Nh . Then, the fundamental frequency is $1 / Nh$. The other frequency components (harmonics) are multiples of the fundamental frequency, $2 / Nh$, $3 / Nh$, $4 / Nh$, etc. until the Nyquist frequency.

The frequency resolution is the difference between two contiguous frequency components. According to the Eq. (3-4), the resolution increases as the sample length increased. If the frequency resolution is too coarse, fine details (peaks) may be lost, however it must be chosen adequately in order not to be undesirable respect to the computational time.

$$\delta_f = \frac{f_N}{\text{number of points in the sample}} = \frac{1}{2Nh} \quad (3-4)$$

3.2.2 Spectral leakage and windowing function

The window function is a smoothing function that solves the problem of the spectral leakage in a discrete sample. In order to understand that function more clearly, the following example has been mentioned by NWM Bishop [9].

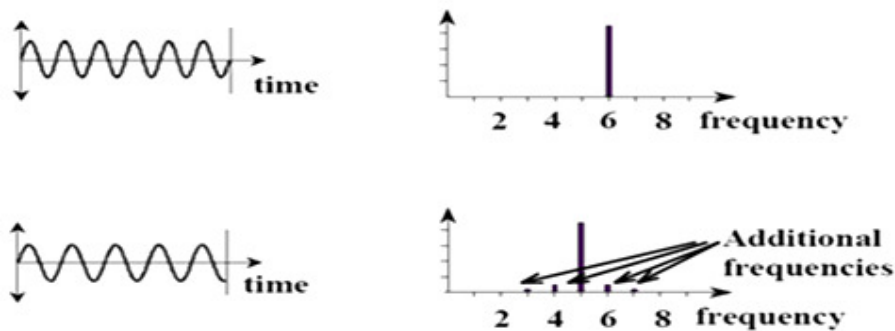


Figure (3-4) Spectral leakage [9]

As an example, if there was a sine wave of a frequency of 6Hz, then by taking a sample length of 1 second there will be 6 complete sine cycles that will be included in the sample. The Fourier spectrum for that wave will be a single spike centered at 6Hz. When the same process is carried for the same sine wave with a 4.8Hz then the FFT will predict that this window is joined to an identical one before and afterwards. This will create extra steps in the continuous function producing additional frequencies and is called the spectral leakage. Figure (3-4) shows this example.

Spectral leakage affects any frequency component of a signal which does not exactly coincide with a frequency channel [29]. The frequency channels are the exact multiples (harmonics) of the fundamental frequency. A sine wave with a frequency coinciding with one of these frequency channels has the property to fit an exact number of sine wave cycles into the complete sampled signal.

Since the frequency components of an arbitrary signal are unlikely to satisfy this condition, it is necessary to reduce the effects of the spectral leakage.

As defined earlier, this is done by the window functions which are smoothing functions that affect the start and the end of the sample by multiplying it with zero and then increase it gradually until it reaches the maximum at the centre [29]. This function

eliminates any possible step in the time function improving the frequency results. Several window functions (Hanning, Hamming and Blackman) are plotted in Figure (3-5). A rectangular window keeps the function with the same conditions.

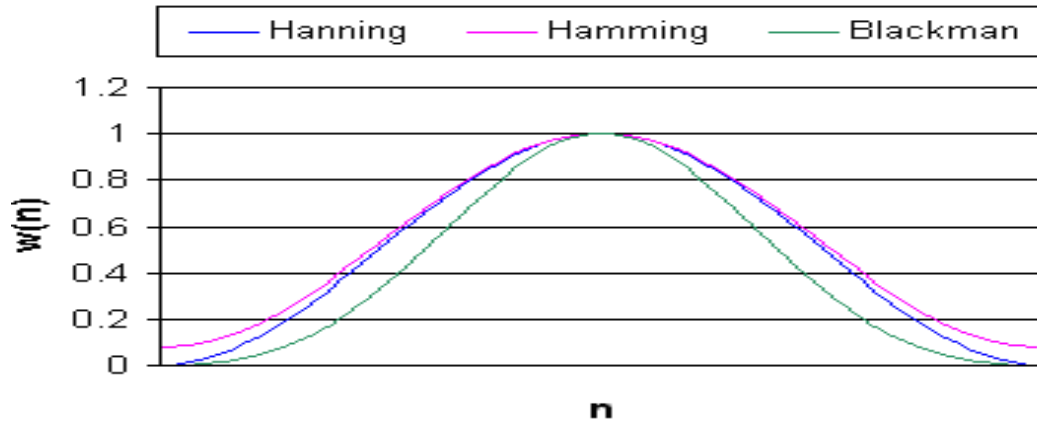


Figure (3-5) Window function- Source [29]

The most common window function is the Hanning window function, which is one cycle of an inverted cosine function scaled to have a maximum value of 1 in the middle and zero at either ends. Figure (3-6) shows this function.

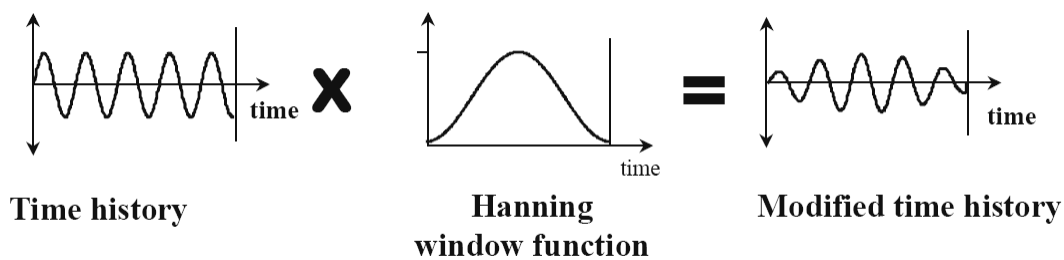


Figure (3-6) Hanning window function [9]

3.3 Power Spectral Density PSD

The term Power Spectral Density (PSD) refers to the variations of a signal in the frequency domain [30]. So, it shows at which frequencies the variations are strong and at which frequencies the variations are weak. It is a useful tool to identify in the time signal, the amplitude at each frequency of vibration.

In a PSD curve, only the amplitude of each sine wave is retained. PSD contains no information about phase relationship between the individual sine waves and without this the time signal cannot be recreated. In the PSD plot the area under each peak represents the mean square of the sine wave at that frequency [11]. This is the reason it is called Mean square spectral density.

PSD is calculated by multiplying the FFT signal by its conjugate. The units of the PSD are G^2/Hz which means that it is the squared value of the FFT.

$$PSD = FFT(f) \cdot FFT(f)^* \quad (3 - 5)$$

If the time signal to be analyzed consists of a finite transient signal, it must be done of energy rather than power spectral densities. This is due to the fact that finite duration time phenomena cannot be characterized by power since power is defined as energy per time.

3.3.1 Characterization of time process using statistical measures

Signals might be described via statistical models as random signals. In the case of random signals it is not possible to predict the way signals change and thus it can only properly be described using statistical analysis. This is because every sample time history is different in the random process. However, since the samples are long the statistics of each sample should be constant.

There are two important parameters to characterize a time process which are the number of zero crossing points and the number of peaks of the signal. The ratio between these parameters is used to calculate the irregularity factor. The irregularity factor is varying in the range of 0 to 1. When the value of the irregularity factor is equal to one then this wave can be called narrow band process. When the divergence from the narrow band increases it makes the irregularity value tending to be zero and the signal become a wide band process [9].

Figure (3-7) refers to one second piece cut out from a time signal. It is possible to calculate the $E[0]$ which denotes the number of the upward zero crossing with the zero line, in the example it is equal to 3. The number of the peaks $E[P]$ is equal to 6. In order to obtain the irregularity factor for the sample shown in the example below then:

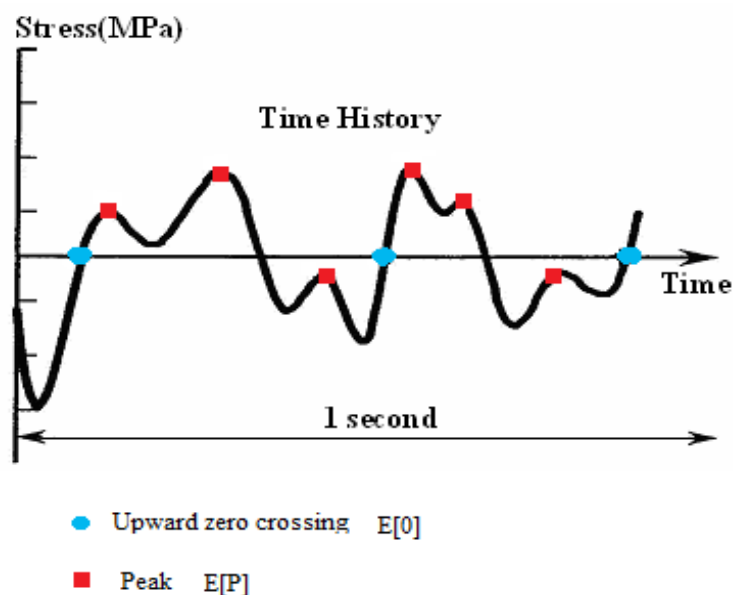


Figure (3-7) Zero and peak crossing rates – source [9]

Number of upward zero crossings $E[0] = 3$

Number of peaks $E[P] = 6$

Then the irregularity factor will be:

$$\gamma = \frac{E[0]}{E[P]} = 0.5$$

The RMS value (Root Mean Square) from the time history curves is a statistical value of the magnitude of the signal [30]. It can be calculated from the time history as the square root of the average of the squares of the signal values.

$$\text{RMS} = \sqrt{\lim_{T \rightarrow \infty} \frac{1}{T} \int_{-T/2}^{T/2} x^2(t) dt} \quad (3 - 6)$$

3.3.2 Characterization of frequency process using statistical measures

Since Spectral density is concerned to analyze signals in the frequency domain, it is necessary to characterize the statistical properties of the time signal from the spectral density function.

In order to obtain the statistical parameters, the moments from the spectral density function are calculated by the following formulation [9].

$$m_n = \int_0^{\infty} f^n \cdot G(f) df = \sum f_k^n \cdot G_k(f) \cdot \delta f \quad (3 - 7)$$

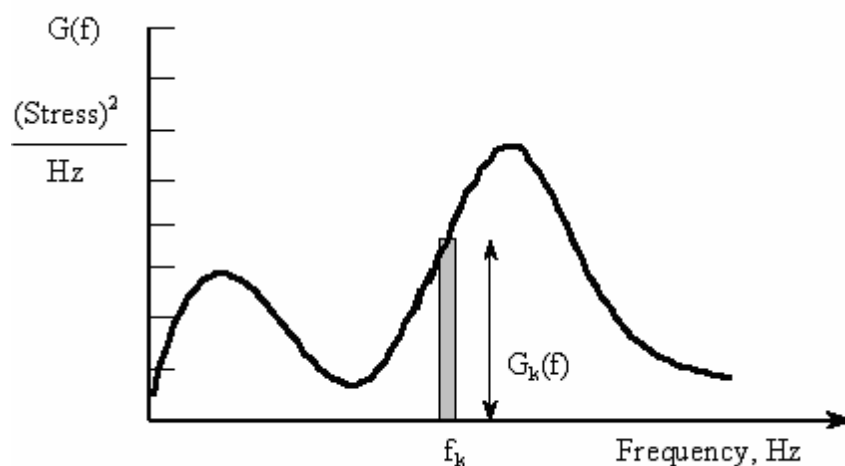


Figure (3-8) Calculation of moments from a PSD – Source [9]

The n^{th} moment of area of the PSD function is calculated by dividing the area under the PSD curve into many bands with a dS width and then multiplying this area by the frequency to the power n . The n^{th} moment of area for the PSD can then be gained by summing up the moments for all the areas as it can be seen in Eq. (3-7) [9].

Once the moments have been calculated, they are used to obtain the irregularity factor and the root mean square value from the signal.

$$E[0] = \sqrt{\frac{m_2}{m_0}} \quad (3 - 8)$$

$$E[P] = \sqrt{\frac{m_4}{m_2}} \quad (3 - 9)$$

$$\gamma = \frac{E[0]}{E[P]} = \sqrt{\frac{m_2^2}{m_0 m_4}} \quad (3 - 10)$$

The RMS (Root Mean Square) in the PSD function represents the average energy of a waveform [30]. It is calculated by equation (3-11).

$$\text{RMS} = \sqrt{m_0} \quad (3 - 11)$$

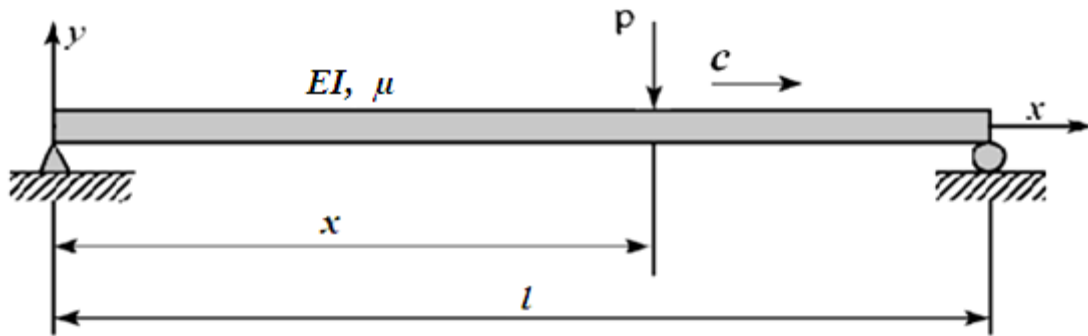
4 Load model

In this chapter the limits for the dynamic effects of a moving load on a beam is discussed.

Based on the results a load spectrum is proposed.

4.1 Moving point load traversing a simply supported beam

A simple supported beam with a concentrated load moving along the beam with a constant speed c , as shown in the Figure (4-1), is studied.



Figure(4-1) Simply supported beam traversed by a moving load with constant speed[19]

The beam deflection at one point as a function of time can be calculated as [19]:

$$w(x, t) = \dots$$

where w_0 denotes the static deflection at mid span of a static force p .

$$w_0 = \dots$$

The angular frequency at the j -th mode of vibration of the beam can be written as.

$$\omega_j = \dots$$

and the circular frequency is denoted as.

$$\omega = \frac{\pi c}{l} \quad (4-4)$$

Before continuing further the speed parameter α_c and the critical speed c_{cr} are introduced.

$$\alpha_c = \frac{c}{c_{cr}} \quad (4-5)$$

$$c_{cr} = \frac{\pi}{l} \sqrt{\frac{EI}{\mu}} \quad (4-6)$$

And D that represents the dynamic deflection at mid span divided by the static deflection at mid span.

$$D = \frac{v\left(\frac{L}{2}, t\right)}{v_0} \quad (4-7)$$

Moving loads have an important effect on all kind of structures. Especially at high speeds, instability can occur. Figure (4-2) shows the deflection at midspan for different load speeds. Although $\alpha_c \ll 1$, it can clearly be seen how the amplitude of the vibration is increased with the speed.

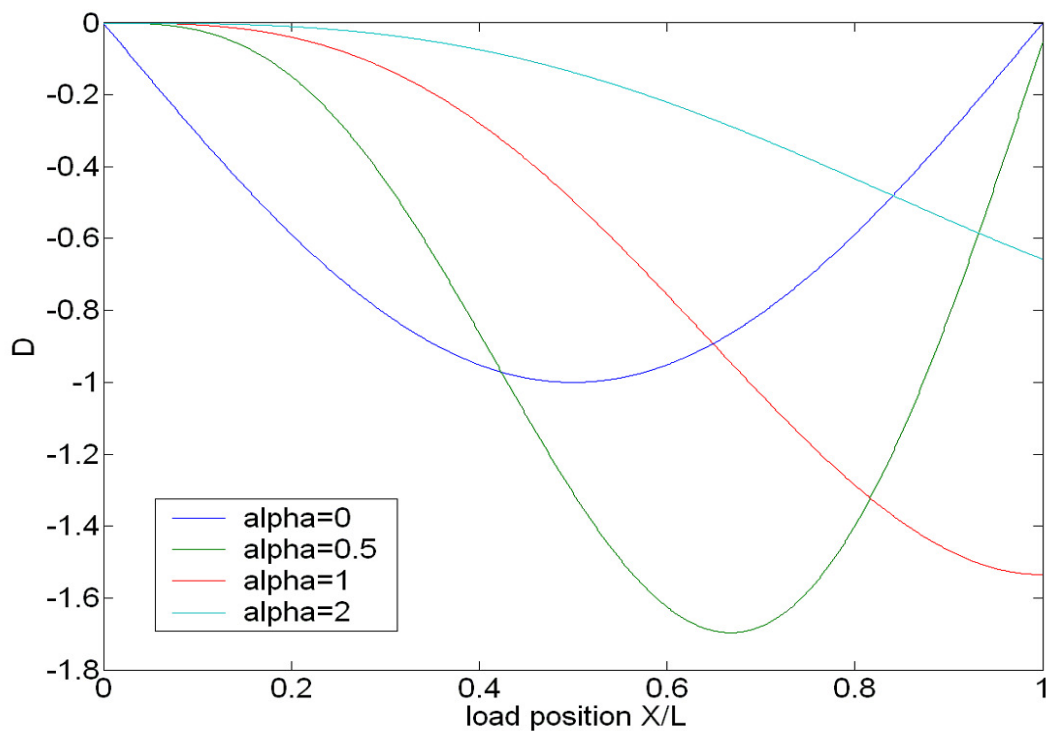


Figure (4-2) Deflection at mid span of the beam for various values of speed

It can be noticed that at subcritical speeds $\alpha_c < 1$, the maximum deflection at mid span is already produced during the load traverse, while at supercritical speeds $\alpha_c \geq 1$, it is produced after the load leaves the beam.

Once the load leaves the bridge, a state of free vibration starts. The attenuation of this phenomenon depends on the characteristics of both the structure and the material [19].

Figure (4-3) shows the maximum deflection at mid span as a function of the speed parameter α_c for beams with various damping values. It can be seen that the deflection appears at α_c in the range of 0.5 to 0.7. For higher speeds the deflection decreases.

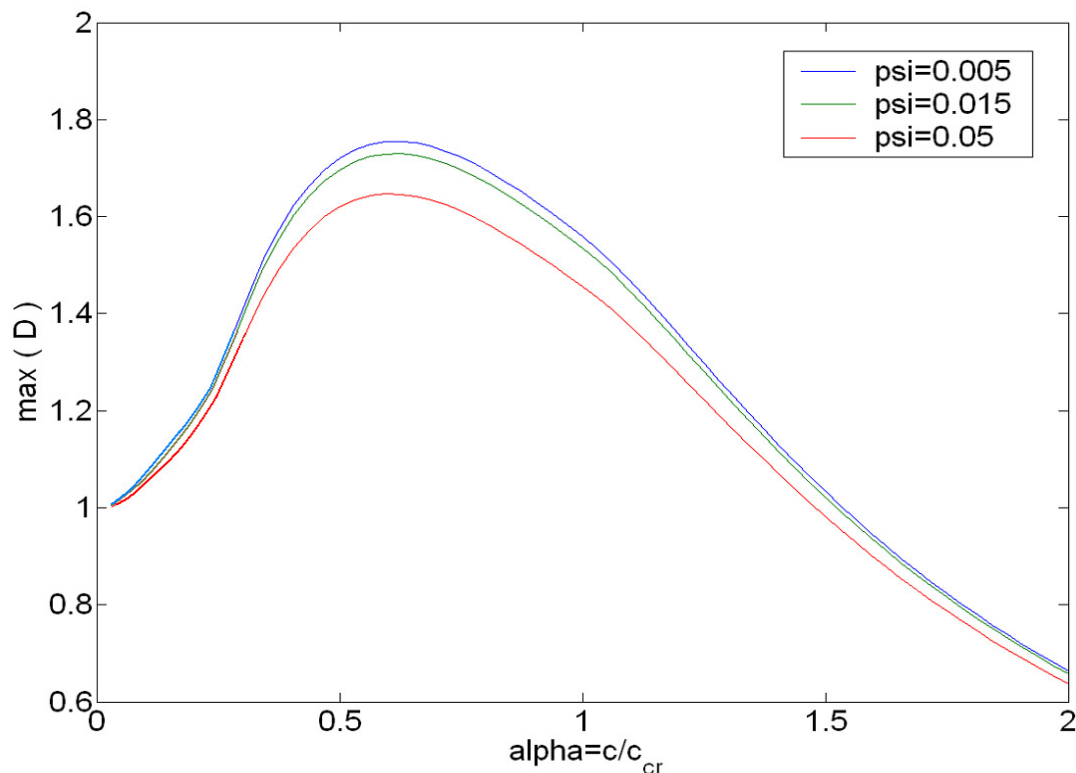


Figure (4-3) Maximum dynamic deflection at mid span of the beam

However, as mentioned in the introduction, the aim is to evaluate the speed limit where the effect of the moving load is relatively small. Examining Figure (4-3), one can see that the dynamic amplification is small for load speeds $\alpha_c \leq 0.1$. For those speeds, the deflection is not far away from the static value.

4.2 The train load

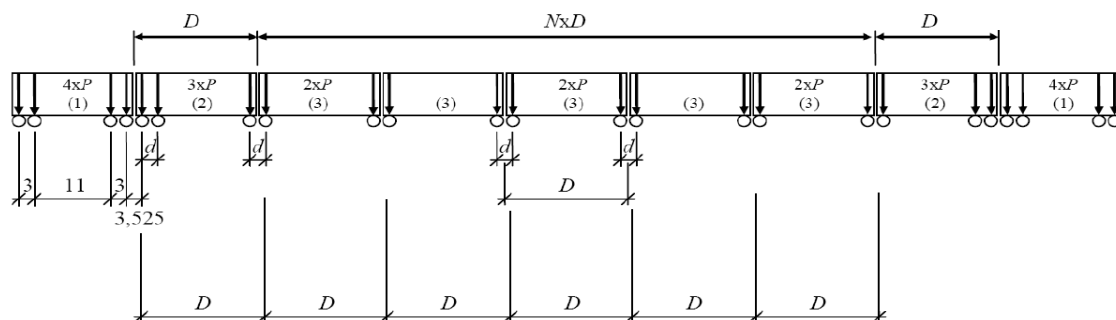
Defining a train load can be tricky, as in a real situation, each train will have its own composition. To adopt a practical approach the Eurocode [13] has been paid attention.

Eurocode defines a train model that can be used to evaluate the dynamic effects of bridges subjected to high-speed train load. The HSLM, High Speed Load Model, consists of two different train configurations, HSLM-A and HSLM-B, with different coach lengths.

In this study, the HSLM-A load model is chosen because its composition has been demonstrated to be an envelope of a variety of European trains [13].

Although the HSLM-A model is designed for high speeds, in this study, it is used as a base and applied to low speeds.

The train configurations are shown in Figure (4-4) and Table [4-1].



- (1) Power Car (leading and trailing power cars identical)
- (2) End coach (leading and trailing end coaches)
- (3) Intermediate coach

Figure (4-4) HSLM-A Load Train Types according to the Eurocode [13]

Table [4-1] Details of HSLM-A trains [13]

Train	Number of intermediate coaches (N)	Coach length (D)	Bogie axle spacing d [m]	Axle load P[kN]
A1	18	18	2	170
A2	17	19	3.5	200
A3	16	20	2	180
A4	15	21	3	190
A5	14	22	2	170
A6	13	23	2	180
A7	13	24	2	190
A8	12	25	2.5	190
A9	11	26	2	210
A10	11	27	2	210

4.3 Relation between geometric dimensions, load speed and Fourier components

A time history of a typical HSLM-train load is shown in Figure (4-5), simulating each of the axel loads in the time domain. Considering a single point on a structure, each axel load is creating a harmonic loading with different frequencies depending on the geometry and the speed of the train.

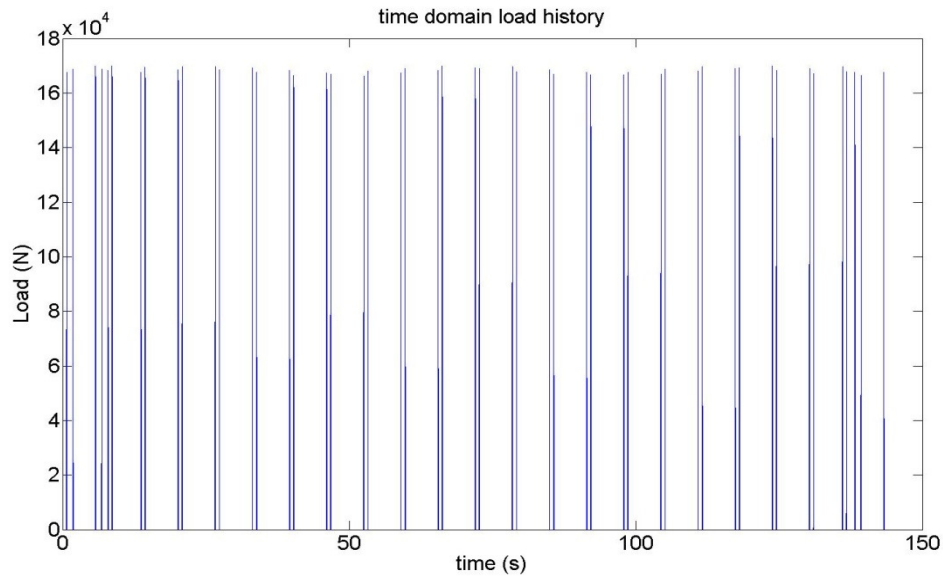


Figure (4-5) Time domain load history of a HSLM-A1 train at 10km/h

As explained in chapter 3, any periodic waveform can be expressed as the summation of number of sinusoidal waves with different frequency and amplitude. Therefore, a periodic waveform consists of one lowest frequency component and multiple of the lowest frequency component. The lowest frequency component is called fundamental frequency and the multiples of the fundamental frequency are called harmonics.

The frequencies the train load model generates depend on the geometry and the speed of the train. The distance between the bogies produce a periodic load with a frequency f and a time period T . The relationship between the frequency f , the time period T , the speed of the train c and the distance between bogies D is shown in Equation (4-8).

$$f = \frac{1}{T} \quad \text{and} \quad T = \frac{D}{c} \quad \text{then} \quad f = \frac{c}{D} \quad (4-8)$$

In order to demonstrate the frequency relationship between the geometry and the speed, two different speeds in the range of 10-50 km/h generated by the HSLM-A1 train are used. For a HSLM-A1 train, the longest distance is $D=18$ m. The load distribution from Figure (4-4) and speeds of 10 and 30 km/h produces frequencies of 0.15 Hz and 0.46 Hz respectively. Figures (4-6) and (4-7) show these fundamental frequencies and the harmonic components $2f$, $3f$, $4f$ and so on, that the load is composed of.

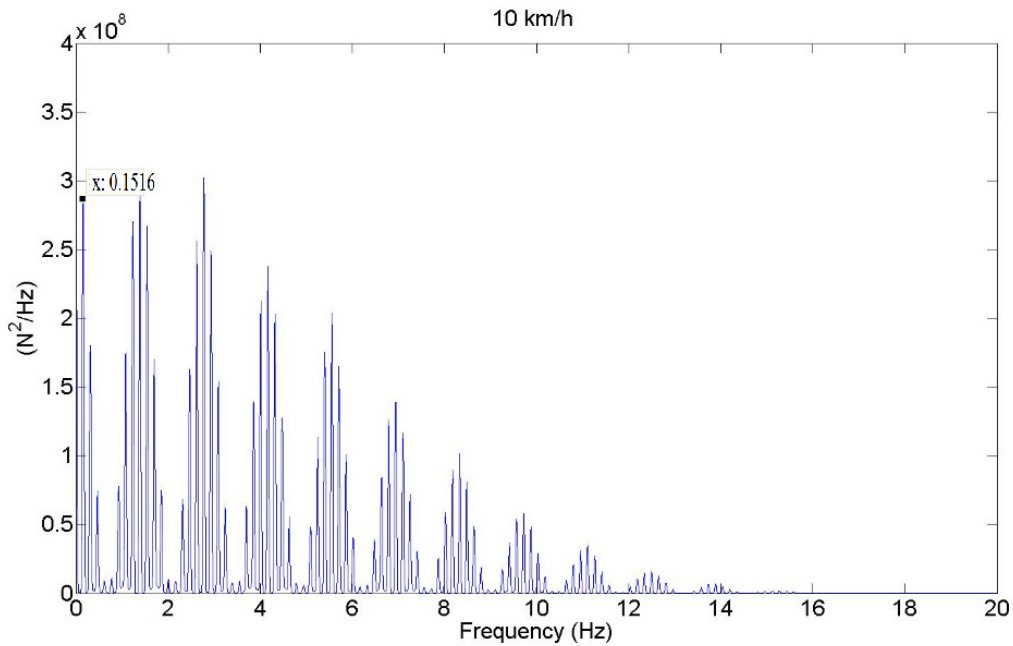


Figure (4-6) PSD load at speed of 10 km/h

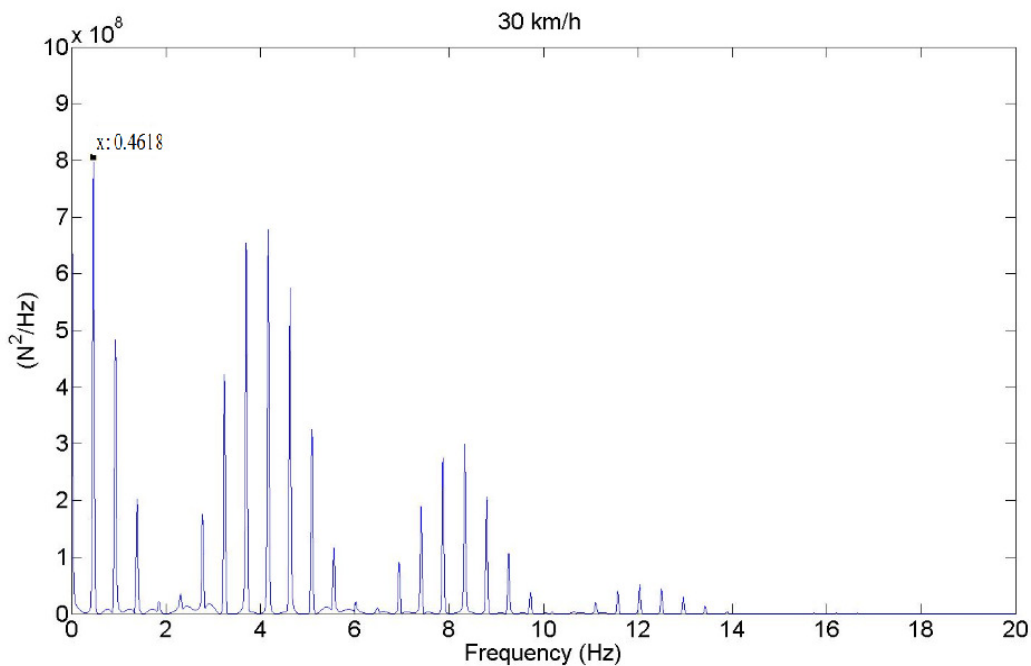


Figure (4-7) PSD load at speed of 30 km/h

4.4 Load in frequency domain

To simulate a realistic case, 10 trains A1-A10 as shown in Table (4-1) with speeds 10 to 50 km/h that vary 5 km/h, are used. Through converting these time signals into the frequency domain by using the Welch's method [27], the result is shown in Figure (4-8). Where x-axis represents the trains (A1-A10), z-axis represents the frequencies that these load models will correspond to. While y-axis represents the load level.

Figure (4-8) shows all spectral components with the considered load and speed range.

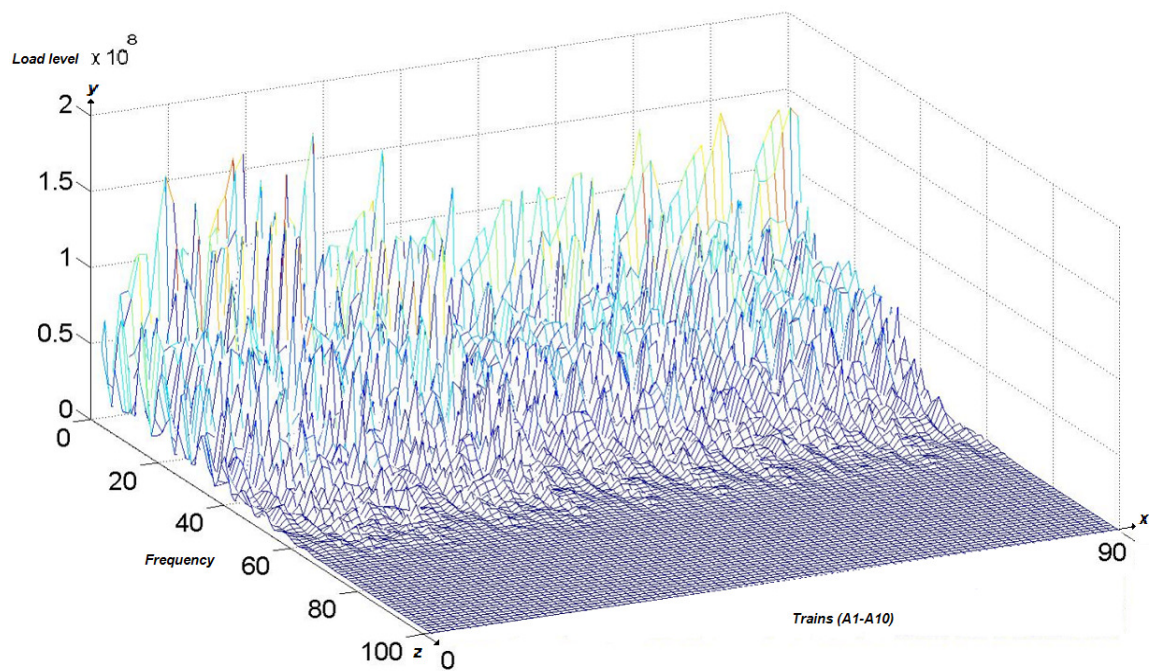


Figure (4-8) All trains load in frequency domain

According to Equation (4-8) and Figure (4-8), it can be noticed that the peaks are moving towards higher frequencies as the speed of the trains increased. In order to understand the speed effect on the frequency, the relation between the speed and the frequency can be presented by Figure (4-9), where the speeds from 10-50 km/h are applied to one train model.

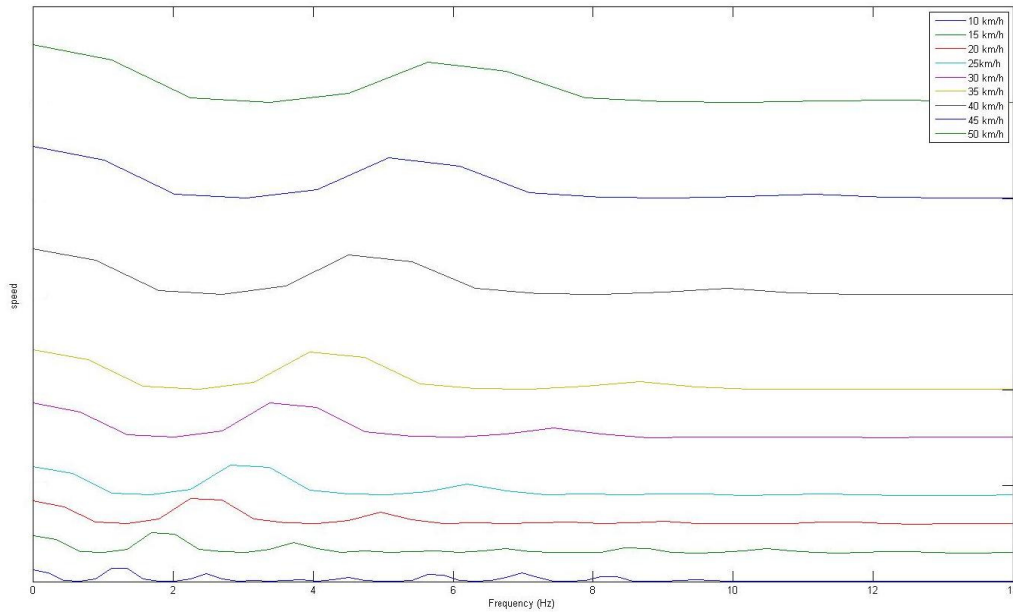


Figure (4-9) Relationship between trains speed and the frequencies

Three different load spectrums are calculated based on the result in Figure (4-8), an averaged, a peak hold and a white noise spectrum and are explained in detail in Table [4-2].

Table [4-2] Comparison between the average, peak hold and white noise load

<i>Averaged load</i>	<i>Peak hold load</i>	<i>White noise load</i>
The average of all the PSD's at each frequency representing the average energy.	The maximum value of all PSD's at each frequency represents the maximum energy.	The RMS value of all trains load represents the average energy in the entire time history.
It is used for representing the energy that is related to the fatigue.	It is used to characterize damage caused by a short duration event (impact).	The system is loaded with the same load level in the whole frequency range.

4.4.1 Averaged load spectrum

An average PSD spectrum is calculated based on the spectra presented in Figure (4-8). To examine the effect of frequency resolution, two curves with the frequency resolution of 0.11 Hz and 0.23 Hz are shown in Figure (4-10). To capture the general characteristics of the load, the frequency resolution should not be too fine. For the purpose of this study the resolution of 0.23 Hz is chosen.

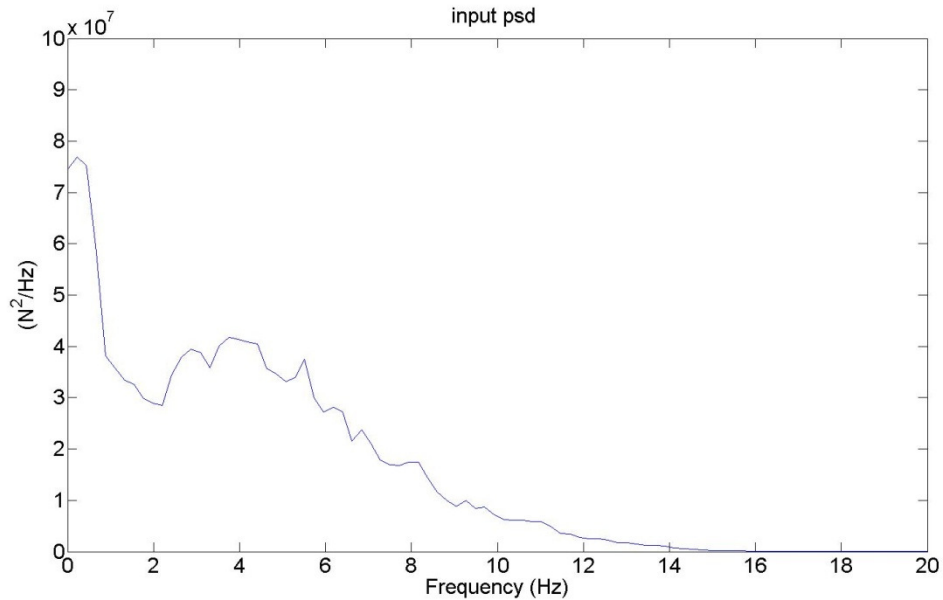


Figure (4-10) Averaged load spectrum with a resolution of 0.2256 Hz

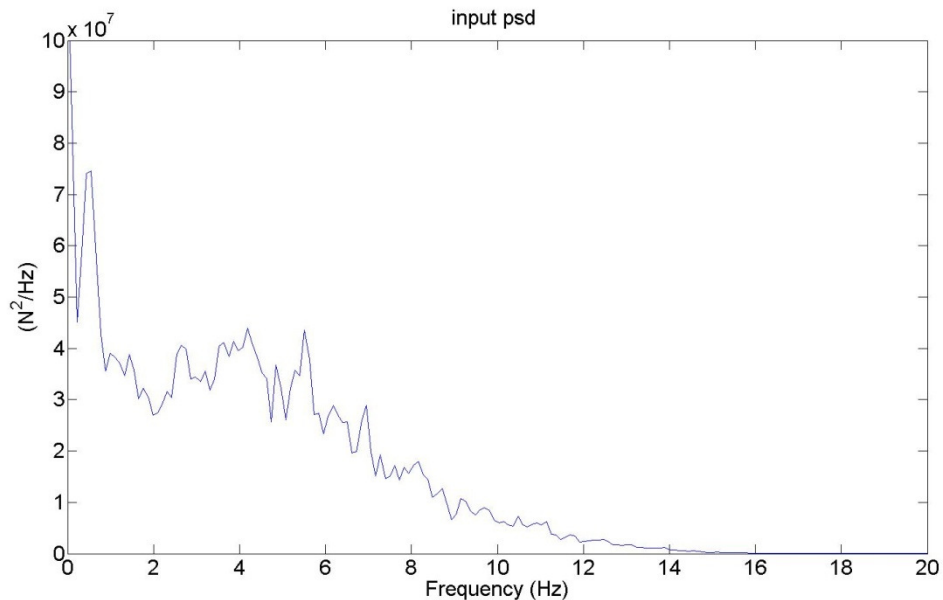


Figure (4-11) Averaged load spectrum with a resolution of 0.1128 Hz

4.4.2 Peak-hold load spectrum

The peak hold spectrum load represents the maximum level among all the trains. Therefore, it can be useful to evaluate, for example, stresses subjected to impact loading. Figure (4-12) shows the difference between the Peak hold and Averaged load spectrum.

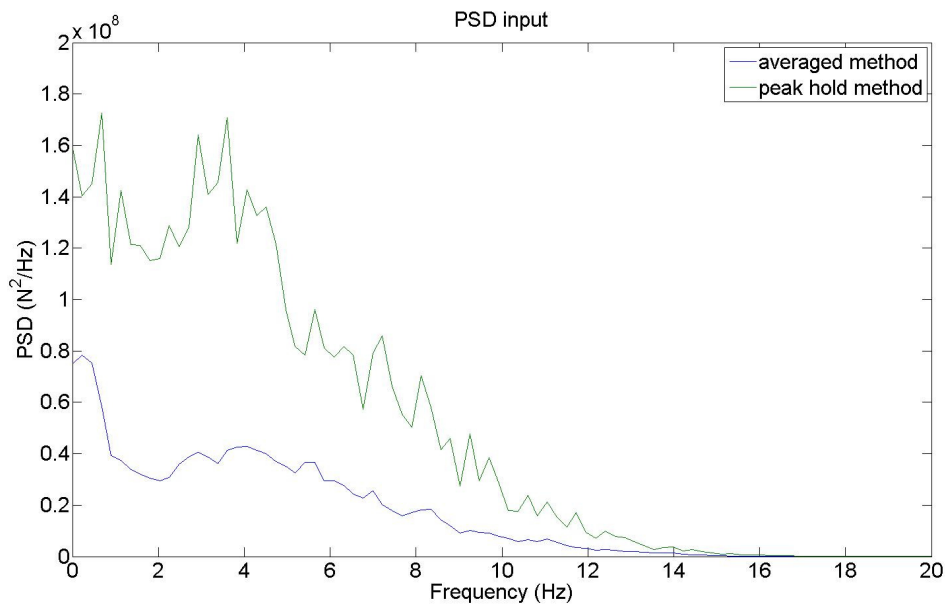


Figure (4-12) Peak-Hold load spectrum

4.4.3 White noise load spectrum

As mentioned in Chapter 3, a white noise signal consists of all frequencies. Figure (4-13) shows the input PSD White noise load.

In this study, the white noise load level will be the RMS of the averaged PSD.

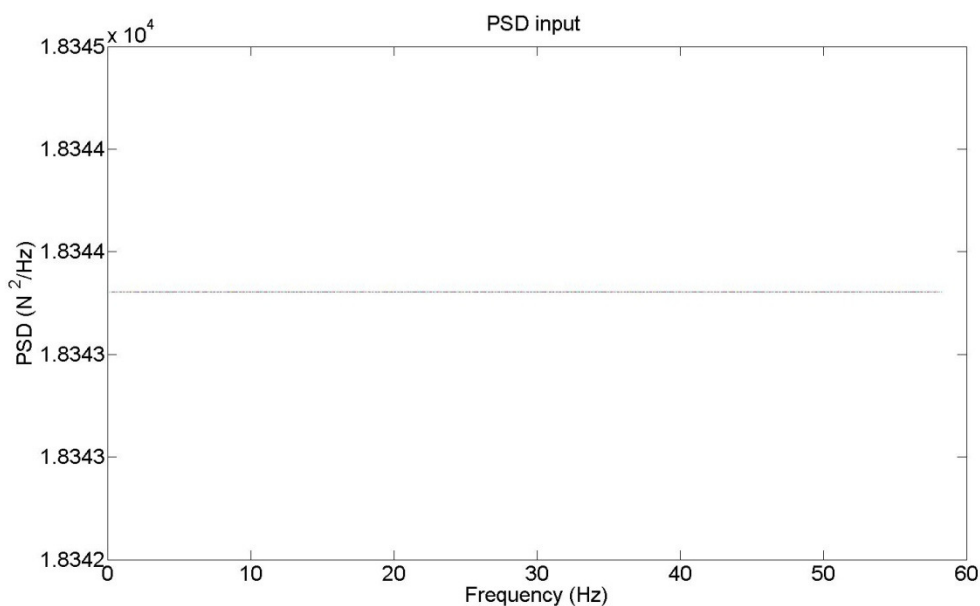


Figure (4-13) White noise load spectrum

5 The SDOF system

In structural dynamics the behaviour of a structure subjected to dynamic loads is evaluated. In this chapter a structure with one degree of freedom (SDOF) is studied. A mass-dashpot-spring system is an example of a single degree of freedom system as shown in Figure (5-1).

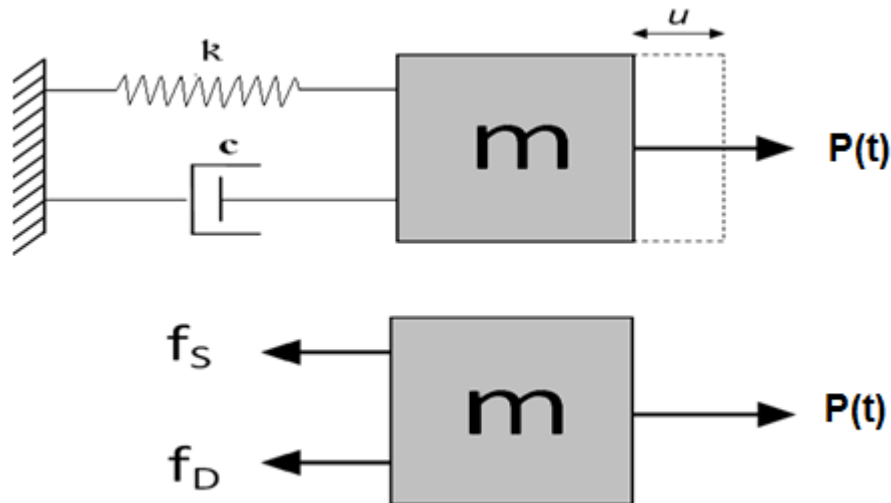


Figure (5-1) SDOF system

In order to determine the response, an analysis is carried out. Equilibrium equations should be satisfied between inertia forces, damping and stiffness forces and the external force. Applying Newton's second law, the equation of motion can be calculated as

$$M \ddot{u} + C \dot{u} + K u = P \quad (5 - 1)$$

Assuming a linear spring K , and a linear damper C , the general solution can be expressed as a sum of a particular solution and a complementary solution.

$$u = u_p + u_c \quad (5 - 2)$$

To study the system behaviour, the natural motion is studied. Natural motion is the solution to the Equation (5-2) with no load applied. In this case, the system characteristic of free vibration is studied and only the complementary solution is of interest. To solve this problem the equation (5-1) is rewritten to:

$$\ddot{u} + 2 \xi \omega_n \dot{u} + \omega_n^2 u = 0 \quad (5 - 3)$$

$$\omega_n = \sqrt{\frac{K}{M}} \quad \text{Undamped natural frequency} \quad (5 - 4)$$

$$\xi = \frac{C}{C_{cr}} \quad \text{Damping factor} \quad (5-5)$$

$$C_{cr} = 2\sqrt{KM} \quad \text{Critical damping coefficient} \quad (5-6)$$

The complementary solution can be written as:

$$u_c(t) = c_1 e^{s_1 t} + c_2 e^{s_2 t} \quad (5-7)$$

The roots of the characteristic equation can be calculated to:

$$s_{1,2} = -\xi \omega_n \pm \omega_n \sqrt{\xi^2 - 1} = -\xi \omega_n \pm i \omega_n \sqrt{1 - \xi^2} \quad (5-8)$$

The system can be divided in three cases depending on the damping factor ξ .

- $0 \leq \xi < 1$ *underdamped*
- $\xi = 1$ *critically damped*
- $\xi > 1$ *overdamped*

The solution varies depending on the damping factor. In our work, however, we deal with civil engineering structures where the damping factor in most cases is less than 10 to 20 %. Therefore, only the underdamped case is studied.

$$\omega_d = \omega_n \sqrt{1 - \xi^2} \quad (5-9)$$

ω_d is defined as the damped natural frequency. Assuming that $\xi \ll 1$, then ω_d can be considered to be equal to ω_n .

The solution to the case of free vibration can then be written as:

$$u(t) = u_c(t) = e^{-\xi t} (c_1 e^{i\omega_n t} + c_2 e^{-i\omega_n t}) \quad (5-10)$$

c_1 and c_2 are determined from the initial conditions of the system.

An important observation can be experienced is that the solution is oscillatory.

In the case of harmonic loading $P = P_0 e^{i(\omega t + \alpha)}$, and stationary conditions, the trial solution is;

$$u(t) = u_0 e^{i\omega t} \quad (5-11)$$

$$\dot{u}(t) = i\omega u_0 e^{i\omega t} = i\omega u(t) \quad (5-12)$$

$$\ddot{u}(t) = -\omega^2 u_0 e^{i\omega t} = -\omega^2 u(t) \quad (5-13)$$

Substituting into equation (5-1) and assuming $\alpha = 0$ results in:

$$-M \omega^2 u + C \omega u + K u = P \quad (5-14)$$

The frequency response in terms of displacement can be written as:

$$u(\omega) = \frac{P}{K + i C \omega - M \omega^2} = \frac{P}{K} \frac{1}{(1 - r^2) + (2\xi r)^2} \quad (5 - 15)$$

where

$$r = \frac{\Omega}{\omega_n} \quad (5 - 16)$$

r is the frequency ratio. When the system is excited at the resonance frequency $\omega = \omega_n$, the response of the system is amplified compared to the static case as it can be seen in equation (5-17) and Figure (5-2).

$$u(\omega_n) = \frac{P}{i C \omega_n} \quad (5 - 17)$$

To study the resonance phenomena, the dynamic magnification factor can be defined as:

$$D(r) = \frac{U(r)}{U_0} \quad (5 - 18)$$

which is the amplified response in relation to the static response.

$$U_0 = \frac{p_0}{K} \quad (5 - 19)$$

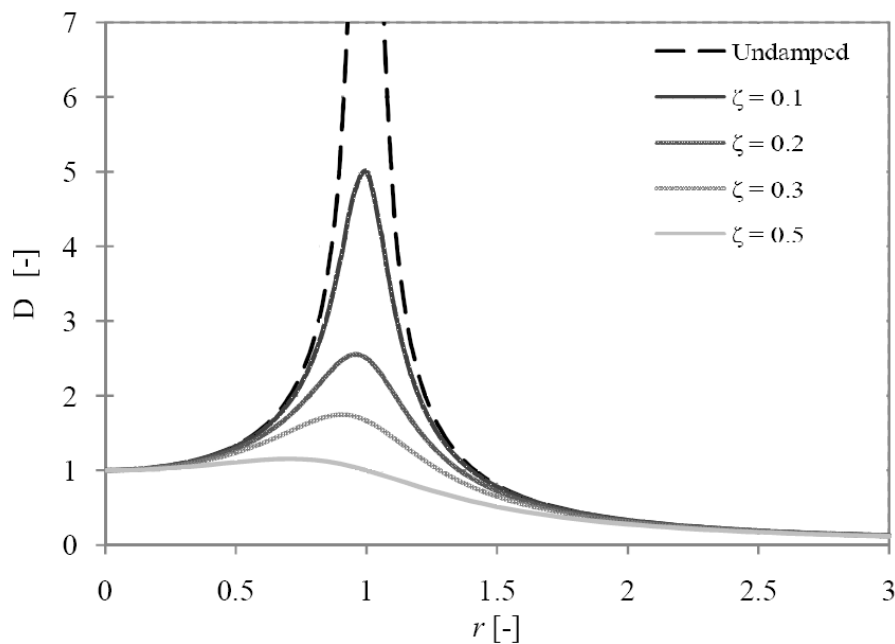


Figure (5-2) Dynamic magnification factor in dependence on damping factor [28]

The dynamic magnification factor as a function of the frequency ratio for different values of the damping factor is shown in Figure (5-2). It can be noticed that higher values of damping imply a lower response of the structure, and resonance phenomena is produced at lower frequencies as the damping factor increases. The dynamic amplification factor is infinite for the undamped system.

6 Vibration fatigue

In civil engineering structures, fatigue damage is often evaluated using S-N curves, where S is fixed amplitude and N is the number of cycles. However, there are many loading scenarios where the loading cannot be determined using single amplitudes. In these cases, the design for fatigue has to be done by using a test based approach or a frequency based fatigue calculation.

With a frequency based fatigue calculation or vibration fatigue approach, a random form of loading can be evaluated by also including the full structural behaviour. In addition, this procedure might be a more computationally efficient procedure than the traditional time domain approach. In Figure (6-2) the methodologies for the time and frequency domain are shown.

6.1 Fatigue life estimation

Equation (6-1) expresses how the fatigue damage is calculated in the vibration fatigue approach.

$$E[D] = E[P] \frac{T}{k} \int_0^{\infty} S^m p(S) dS \quad (6 - 1)$$

This equation determines the fatigue damage in seconds for a detail that is subjected to a stress range S with a probability $p(S)$ by choosing T to be one second. The fatigue life expressed in seconds is calculated by taking the inverse of the damage per second [9].

The constants k and m are derived from the detail category and the S-N curves ($k = N S^m$). These curves are shown in Chapter 2. A linear relationship between cycles to failure N and applied stress range S under constant amplitude cyclic load is observed. Unfortunately, this situation rarely happen in reality, so to calculate the damage caused by stress with a variable amplitude, the concept of a probability density function is introduced.

6.2 Probability density function PDF

The probability density function (pdf) is a statistical measurement that defines a probability distribution for a random variable. The reason this function can be used in the vibration fatigue evaluation procedure is that the stress range histogram data can be expressed in the form of a probability density function.

In order to obtain pdf from a Rainflow histogram chart, each bin in the Rainflow has to be multiplied by the function of ($S_t * dS$). Where S_t represents the total number of cycles

in histogram and dS is the interval width. Then, the probability of the stress ranges $p(S_i)dS$ between $S_i - \frac{dS}{2}$ and $S_i + \frac{dS}{2}$ can be calculated [9].

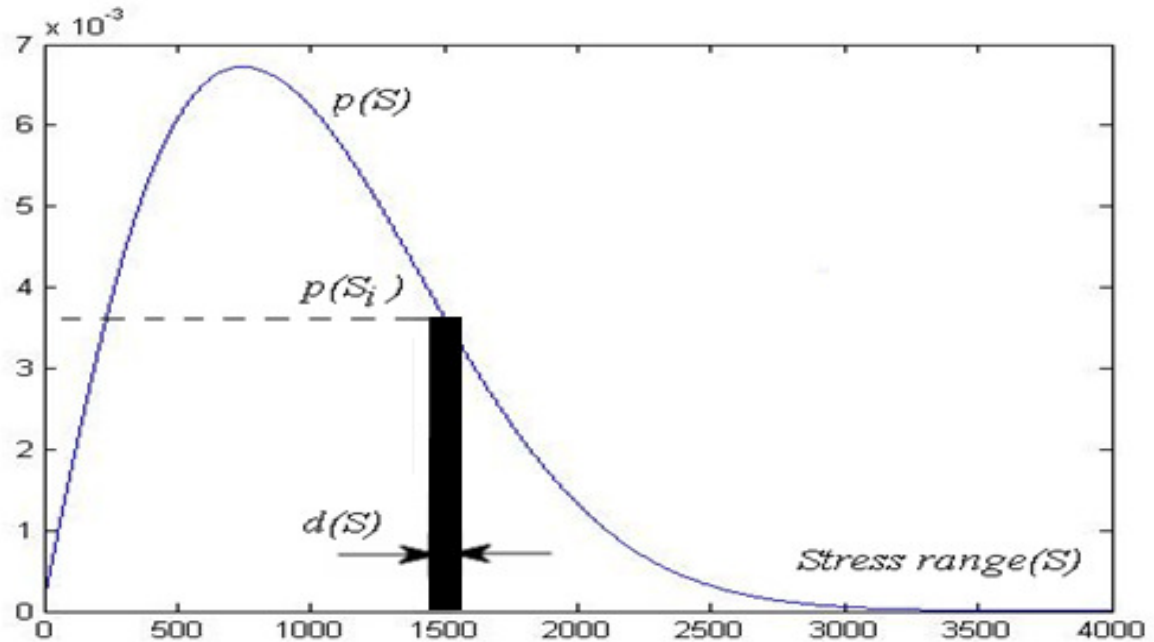


Figure (6-1) Probability density function

Depending on the load characteristics, different methods can be used to calculate the probability density functions. In this thesis two methods are discussed, the Narrow band solution and Dirlik empirical solution.

6.2.1 Narrow Band solution

The Narrow band solution is a conservative approach to design the fatigue life. However, this solution is only suitable for narrow band processes. In our case, we are studying a broad band process. Therefore, the Narrow band solution results in higher stress range and thus a shorter fatigue life.

The reason behind the conservation is that in the narrow band case, the positive troughs and the negatives peaks are not considered. Beside the positive peaks are matched with the corresponding troughs of similar degree in spite of whether they actually form stress cycles or not [9].

In Figure (6-2.c) a cycle is made with every peak by joining it with an imaginary trough at an equal distance the other side of the mean level. It is easy to observe how the bold signal is transformed in the grey signal with higher stress ranges by application of the narrow band method.

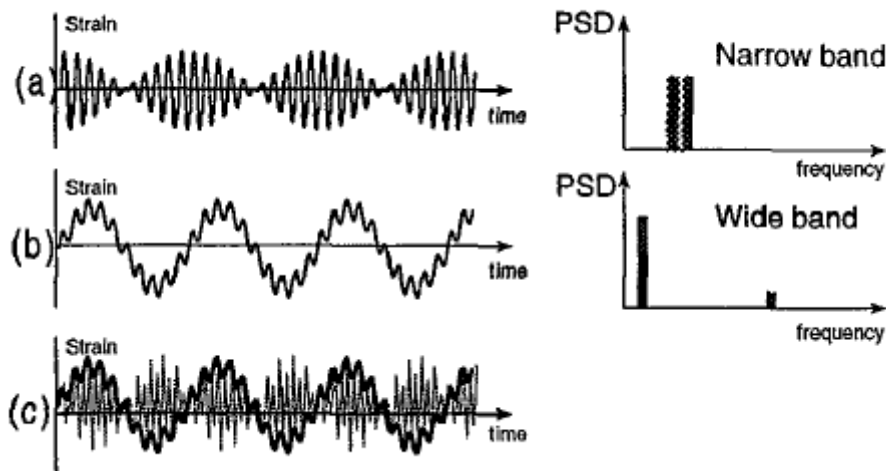


Figure (6-2) Explanation of narrow band solution[9].

The Narrow Band approach assumes that the pdf for the peaks is equal to the pdf of the stress amplitudes, so the Rayleigh pdf of peaks is substituted with the pdf from the stress amplitudes. This is done by considering that S_t is equal to $E[P] T$ [9], where $E[P]$ is the number of peaks. Equation (6-2) calculates the damage by using the pdf that has been extracted from this approach.

$$E[D] = \sum_i \frac{n_i}{N(S_i)} = \frac{S_t}{k} \int S^b p(S) dS = \frac{E[P] T}{k} \int S^b \left[\frac{S}{4 m_0} \exp\left(\frac{-S^2}{8 m_0}\right) \right] dS \quad (6-2)$$

There are many empirical correction factors that have been proposed based on using the Inverse Fourier Transform function to form a time history from the PSD. Tunna, Wirsching, Hancock, Chaudhury and Dover are all methods that use the spectral moments to give more accurate results.

6.2.2 Dirlik empirical solution

Dirlik could construct an empirical form for the pdf of the stress range, by means of extensive computer simulations to shape the signals by using the Monte Carlo approach (Computational algorithms that rely on repeated random sampling to compute their results).

Bishop and Sherratt (1989, 1990) [10] were the first who verify this method theoretically based on the Rainflow counting method.

Dirlik method defines the cycles range distribution by combining two Rayleigh distributions (continuous probability distribution), where the first distribution is to estimate the low amplitude cycles while the second one estimates high amplitudes cycles.

Dirlik proposed his method to approximate the probability density function of the stress ranges which is intended to be valid for both narrow and broad band signals. See Equation (6-3)

$$p(S) = \frac{D_1 e^{-\frac{Z}{Q}} + \frac{D_2 Z}{R^2} e^{-\frac{Z^2}{2R^2}} + D_3 Z e^{-\frac{Z^2}{2}}}{2(m_0)^{1/2}} \quad (6-3)$$

where

Mean frequency

$$X_m = \frac{m_1}{m_0} \sqrt{\frac{m_2}{m_4}} \quad (6-4)$$

Normalized stress range

$$Z = \frac{S}{2 m_0^{1/2}} \quad (6-5)$$

Empirical weight factors

$$D_1 = \frac{2(X_m - \gamma^2)}{1 + \gamma^2} \quad (6-6)$$

$$D_2 = \frac{1 - \gamma - D_1 + D_1^2}{1 + \gamma^2} \quad (6-7)$$

$$D_3 = 1 - D_1 - D_2 \quad (6-8)$$

$$R = \frac{\gamma - X_m - D_1^2}{1 - \gamma - D_1 + D_1^2} \quad (6-9)$$

$$Q = \frac{1.25(\gamma - D_3 - D_2 R)}{D_1} \quad (6-10)$$

The analysis done by Dirlik approach depends on the signals that have been transformed from the time domain to frequency domain and based on the m_0 , m_1 , m_2 and m_4 moments of the PSD function. The results will be gained faster than the Rainflow counting method when summing a random loading over a large time history.

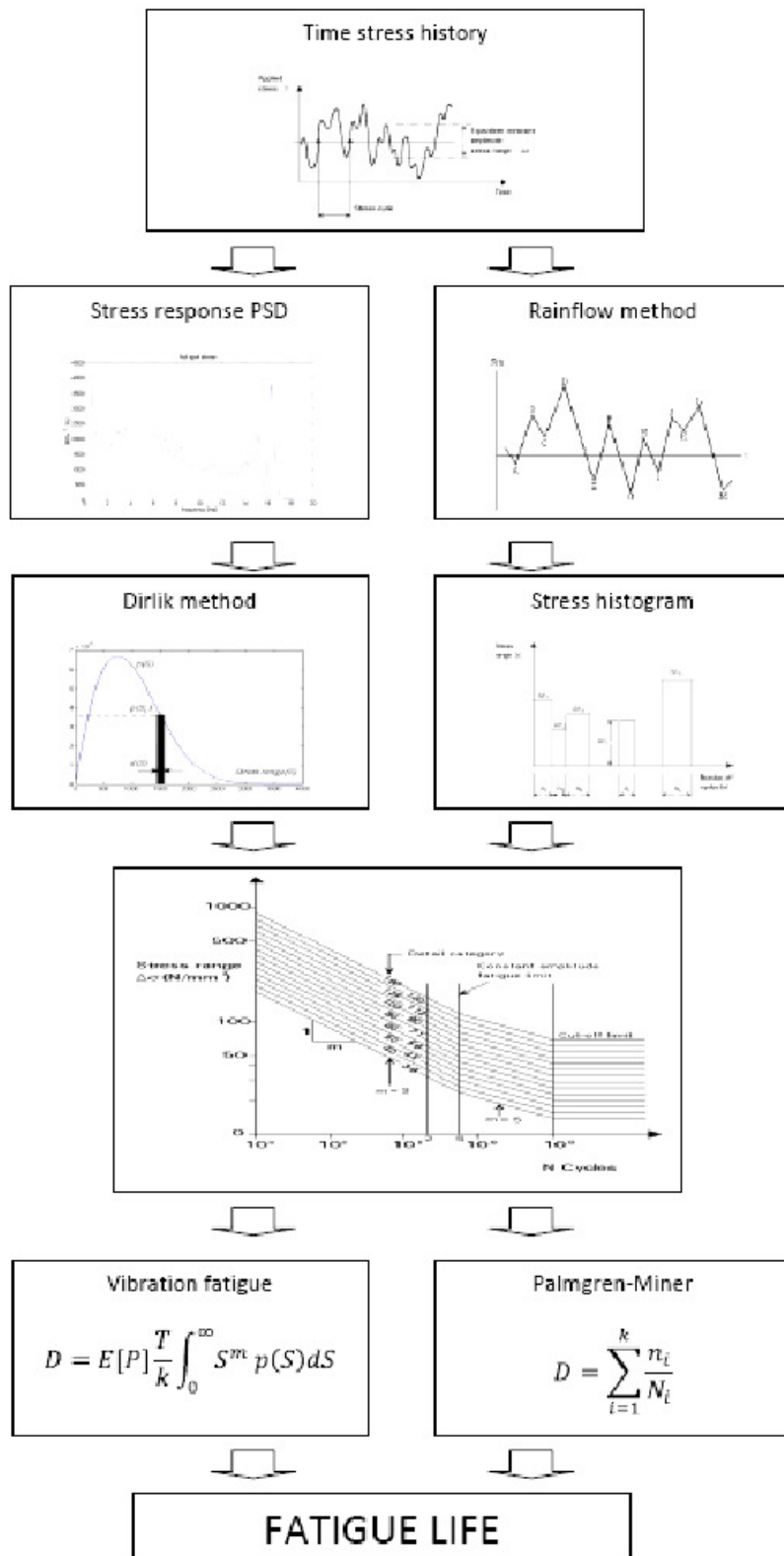


Figure (6-2) Fatigue life estimation schema

7 FE Modeling

In order to study vibration fatigue and explore if a vibration fatigue approach could be used, a detail for the Söderström Bridge was chosen, see figure (7-1). A main beam/cross girder connection from this bridge has been model with Finite Element Method, where cracks were observed.



Figure (7-1) the cracks that were discovered in 1990 [17]

7.1 FE modelling of the detail from the bridge

The Finite Element Modelling (FEM) was performed for the chosen detail using the software ABAQUS 6.8 [20].

The material for the model used was isotropic steel with a modulus of elasticity of 210 GPa, density of 7850 Kg/m³ and Poisson ratio set to 0.27.

The model consists of one main girder with a length of 6.736 m with two vertical stiffeners at both sides of the web. The main girder is connected to a transversal beam of 5.1 m length. The boundary conditions set to be totally fixed along the cross section of the main girders edges.

There are rectangular solid connectors between the stiffeners and the upper flange of the main girder. The dimensions of the connectors are 50x35x200 mm for the inner side while for the outer side was 50x35x120 mm. The numerical model is shown in Figure (7-2).

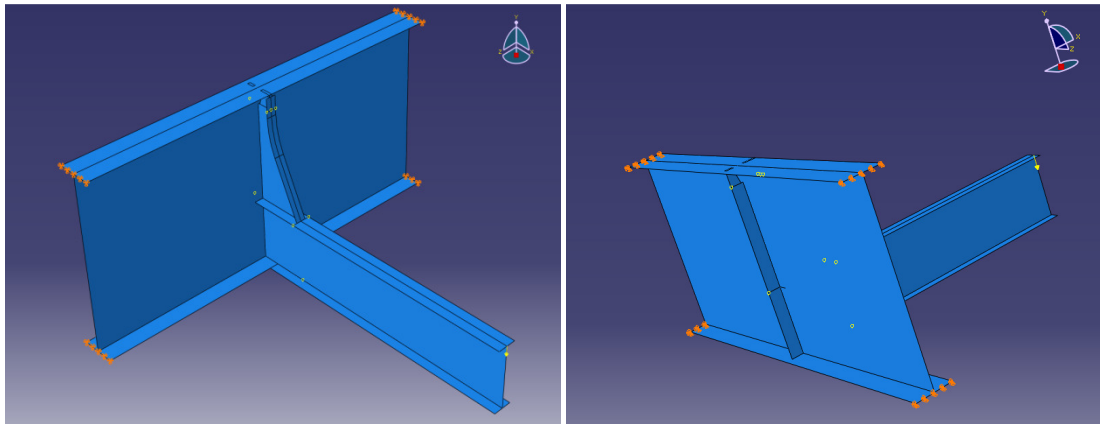


Figure (7-2) A geometrical model of the bridge detail (The red marks represents the boundary conditions).

A modal damping ratio of 1.5% has been adopted for this model, which allows defining a damping factor for the material in the model as a fraction of the critical damping.

Standard linear 4-nodes shell elements were used, except for the connectors that have been modeled with standard linear 8-nodes solid elements. The solid elements try to simulate the stress distribution through the plate thickness.

In the real detail, all parts are welded except for the connectors at the upper flange of the main girder. The bottom part of the connectors is welded to the stiffener. In order to simulate this in the model, a constraint application has been used. The constraint application in ABAQUS allows connecting the shell elements to the solid elements through the shell to solid coupling option [20].

As stated above, the upper part of the connectors in the real detail is not welded to the upper flange. To model this behaviour, contact elements were used.

The gap between the stiffener and the web which can be seen in Figure (7-1) has been modeled in a way that the stiffeners cut off margins could not penetrate the main girder web. This is modeled with the interaction application in the modeling process. For the parts that share surfaces, surface to surface application is chosen, while for the parts that are sharing nodes and surfaces a node to surface interaction application has been chosen.

The load, both static and dynamic, is applied at the end point of the upper flange of the transversal girder as shown in Figure (7-2).

The aim is to study the fatigue life of the detail using the hot spot method. It is important to have a suitable mesh size for the area where the stresses of interest are found. Therefore, main girder region close to stiffeners is of interest.

In order to choose reasonable mesh size for the specific area, a convergence study was conducted using four different mesh sizes. The convergence study can be shown in Figure (7-3).

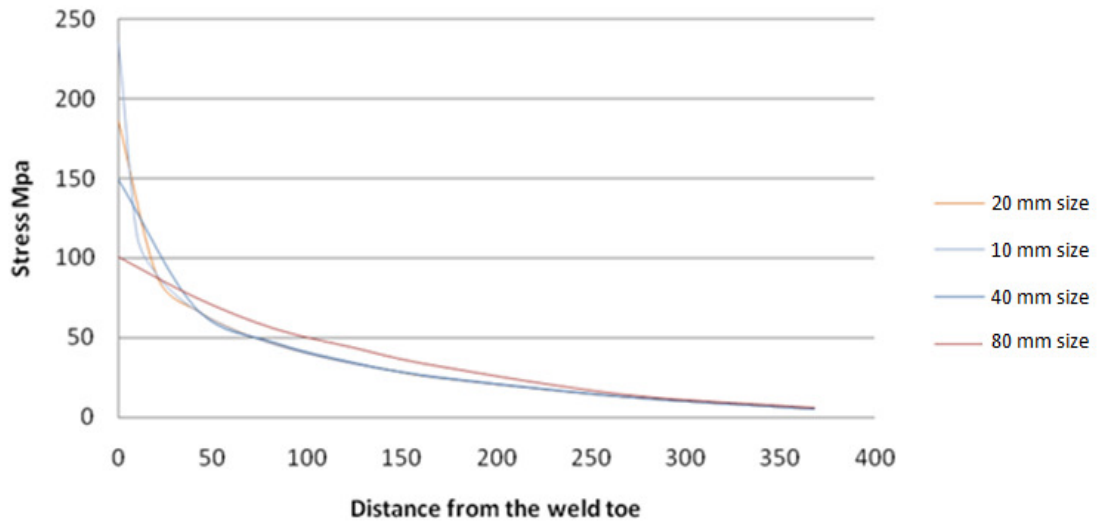


Figure (7-3) The convergence study for choosing the right mesh for the hot spot area in the model.

For the convergence study a vertical path is taken perpendicular to the weld toe in the unstiffened web gap, where the highest deformation is produced. The element sizes applied in the study are approximately 80, 40, 20 and 10 mm. The stresses are produced by a static point load of 100 kN applied at the end of the transversal girder.

The results in Figure (7-3) show that from a hot spot point of view, an element size of 10 mm is adequate for the region of interest. For the rest of the model a more coarse mesh is chosen. Figure (7-4) shows the final mesh for the area of study.

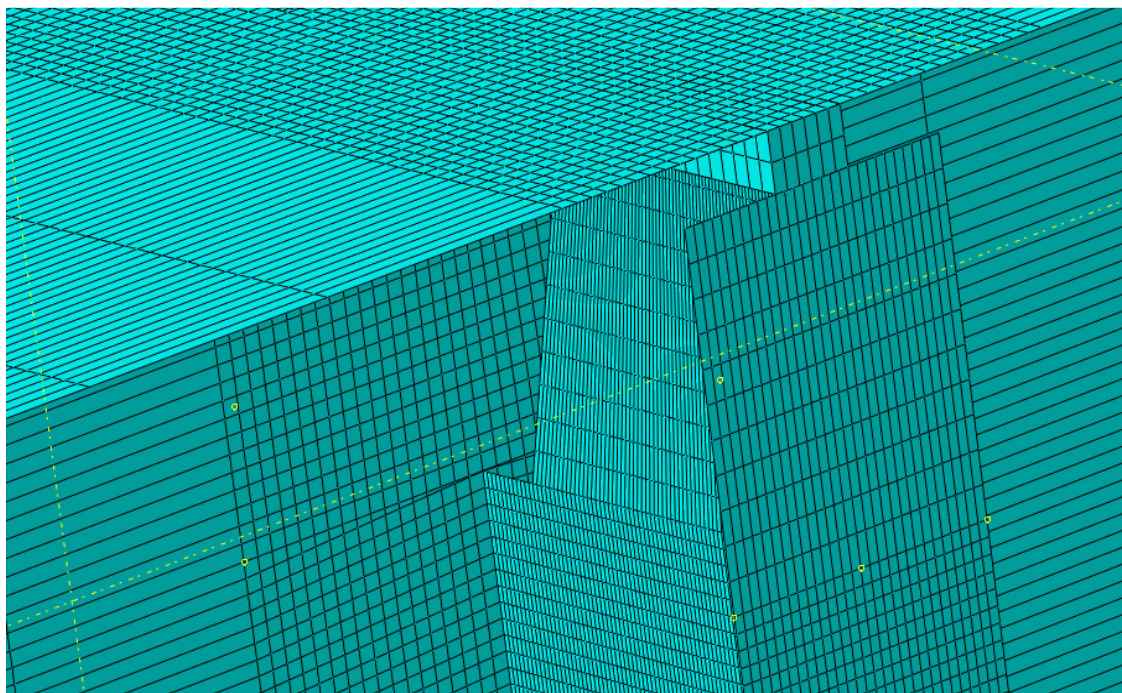


Figure (7-4) the final mesh for the area of study

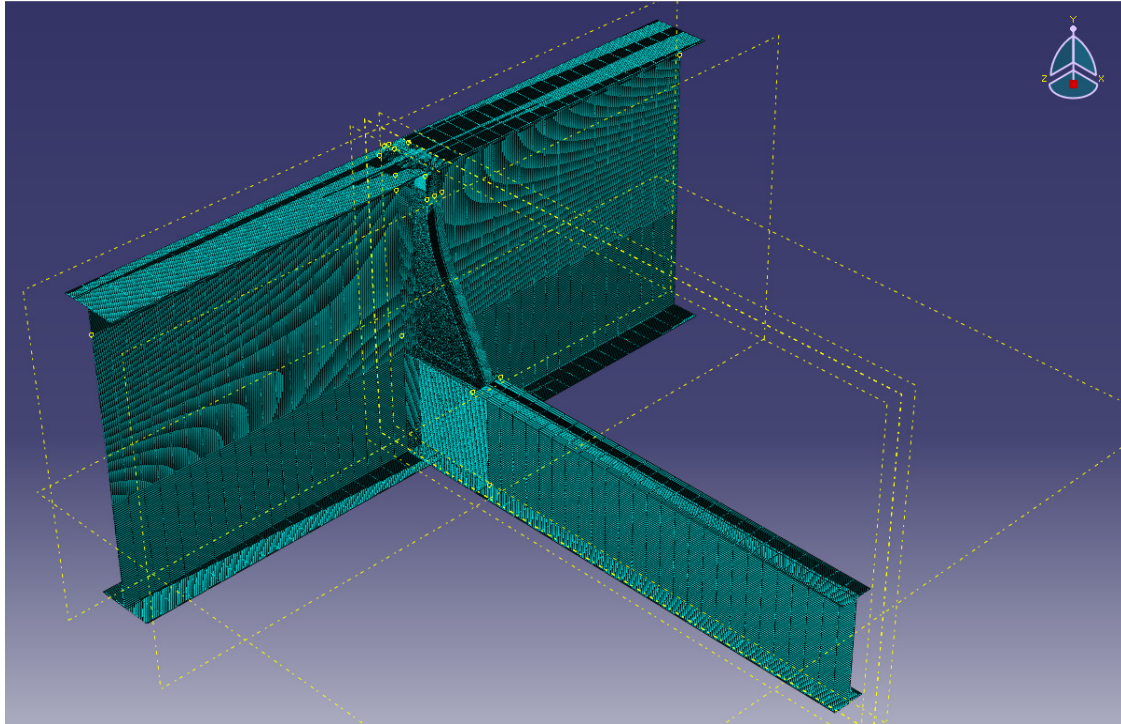


Figure (7-5) the final mesh of the detail

7.2 Structural response of the detail

In order to study the dynamic behavior of the detail, it is necessary to determine its vibration characteristics. Therefore, fundamental characteristics of the structure such as eigenfrequencies and eigenmodes are determined. In addition, a frequency response function is calculated.

7.2.1 Natural frequencies and mode shapes

Natural frequencies of vibration and the corresponding mode shapes of the structure are extracted. ABAQUS provides several eigenvalue extraction procedures. In this study the Lanczos eigensolver is implemented.

For the Lanczos method it is necessary to provide the maximum frequency of interest or the number of eigenvalues required.

The eigenvalue problem for natural modes of vibration of a finite element model is

$$(\mu^2[M] + \mu[C] + [K])\{\phi\} = 0 \quad (7 - 1)$$

where:

$[M]$ is the mass matrix.

$[C]$ is the damping matrix.

$[K]$ is the stiffness matrix.

μ is the eigenvalue.

$\{\emptyset\}$ is the eigenvector—the mode of vibration.

The Lanczos procedure consists of set of Lanczos “runs,” in each of which a set of iterations called steps is performed. The problem allows rapid convergence to the desired eigenvalues [20].

The results from the modal extraction are presented in Table [7-1] and the first six mode shapes are shown in Figure (7-6).

Table [7-1] Eigenfrequency extraction

Eigenmode (N°)	Frequency (Hz)	Mode type
1	5.319	Torsional
2	11.814	Torsional
3	15.367	Bending
4	15.608	Torsional
5	16.348	Bending
6	24.012	Bending

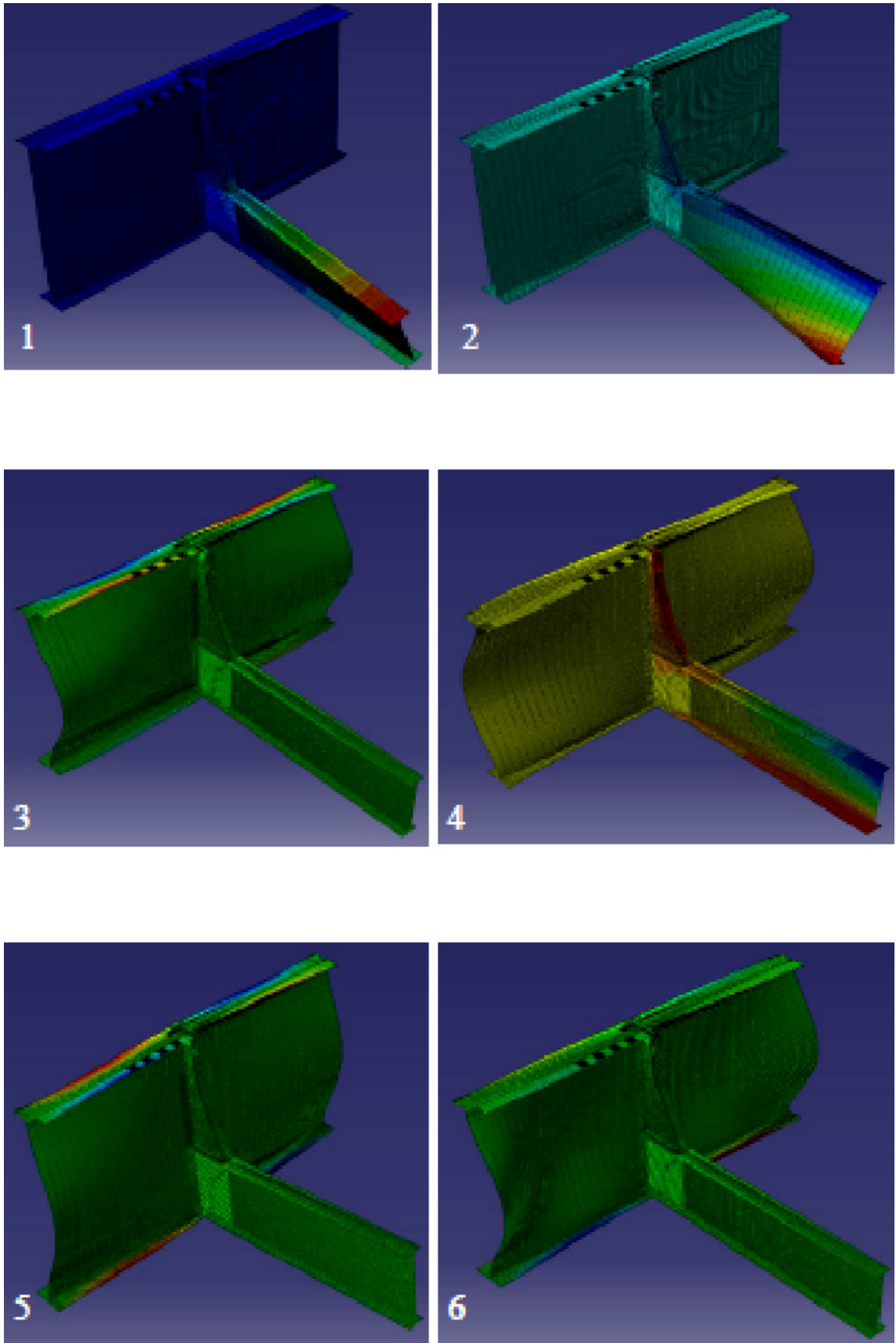


Figure (7-6) Mode shapes for the first 6 modes. $f_1=5.319$ Hz, $f_2=11.814$ Hz, $f_3=15.367$ Hz, $f_4=15.608$ Hz, $f_5=16.348$ Hz, $f_6=24.012$ Hz.

7.2.2 Frequency response analysis

The structural response is studied in the frequency domain. Therefore, the so called frequency response function has to be calculated.

The steady-state dynamic analysis in ABAQUS provides the response of a system due to harmonic excitation at a given frequency. In general, this analysis is done as a frequency sweep, by applying the load at a series of different frequencies and then records the response [20].

The steady-state harmonic response is calculated directly in terms of the physical degrees of freedom of the model using the mass, damping and stiffness matrices of the system, as described in the general equation of motion (5-1) [20].

Based on this analysis, it can be observed that the response is amplified when the system is subjected to a resonance frequency, as it can be seen in Figure (7-7). This principal behavior has also been discussed in chapter 5.

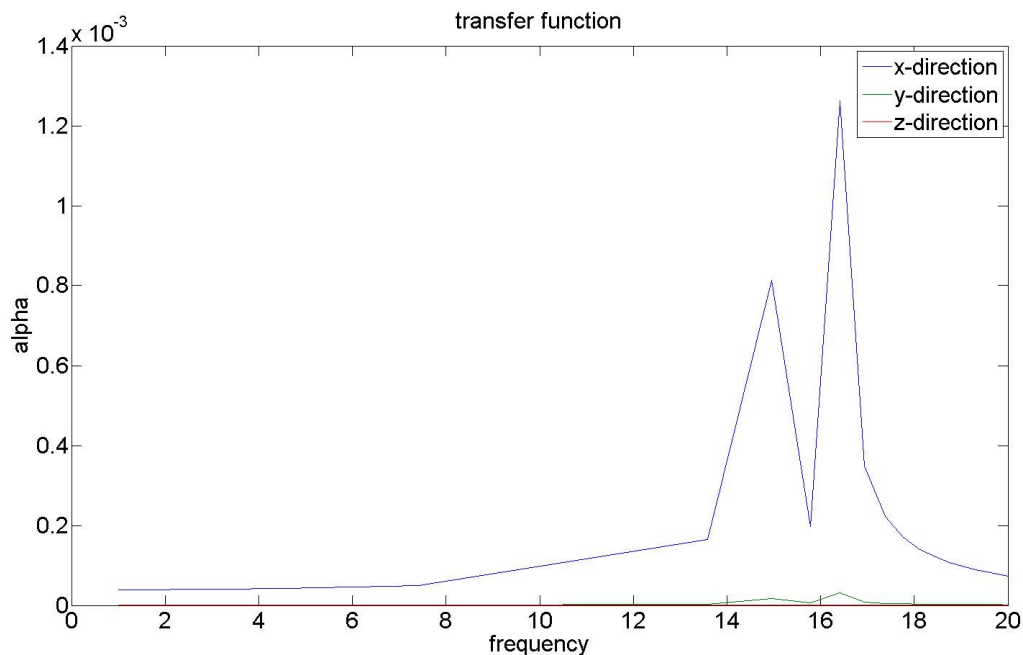


Figure (7-7) Frequency Response Function FRF.

This analysis response is called Frequency Response Function (FRF) and can be defined as a transfer function where there are real and imaginary complex values. Theoretically, the FRF is used to convert the spectral density function of the load into a spectral density function of the response in terms of displacement, strain or stress.

The response of the structure is different in different directions. In the case of the actual model, the FRF differs according to the direction of the displacement chosen. The FRF function has been defined at the upper meeting point between the inner stiffener and the main girder web. This point represents the critical point in the structural detail due to the high deformation caused by the load.

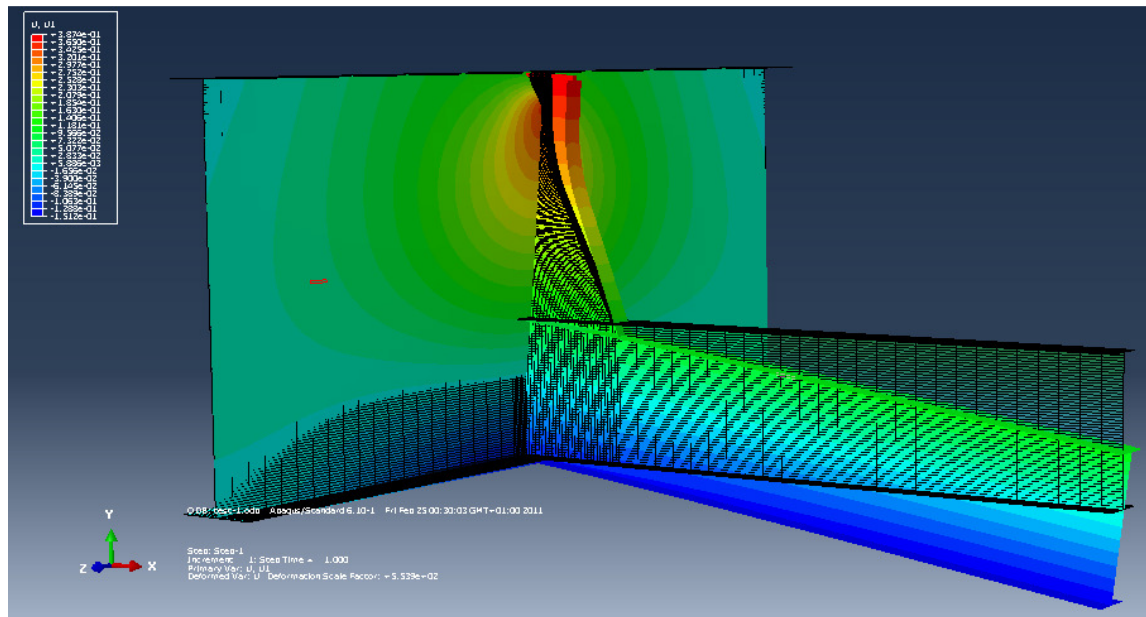


Figure (7-8) U1 displacement for the detail

Figure (7-7) shows the FRF for x , y , and z directions and indicates that the maximum response is for the x -direction. Therefore, it can be justified by referring to Figures (7-8) and Figure (7-9) where the system of study is loaded in the y -direction, representing the train wheels load on the bridge. This load produces a bending moment (M_z) which causes the critical point to deform in the x -direction. This effect causes a higher response in the x -direction comparing by the other directions. Figure (7-8) shows that the maximum displacement in x -direction for the detail occurs in the critical point.

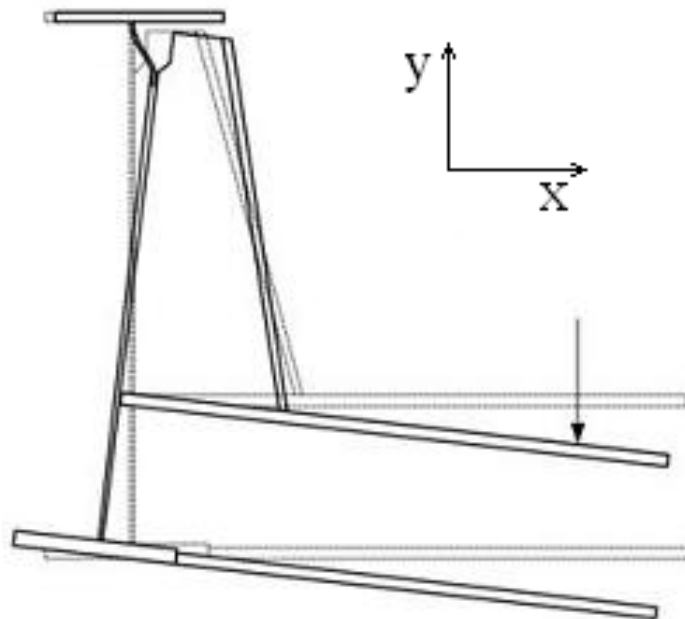


Figure (7-9) Deformation shape for the detail

8 Results

A frequency domain approach was chosen to evaluate fatigue life. First, the PSD of the load was created, then structure was modelled using numerical techniques (FEM) and the FRFs of interest were established.

The load was applied and a random response analysis was concluded. Stress evaluation according to the hot-spot method was used to obtain the stress curves.

A flow chart of the procedure is shown in Figure (8-1).

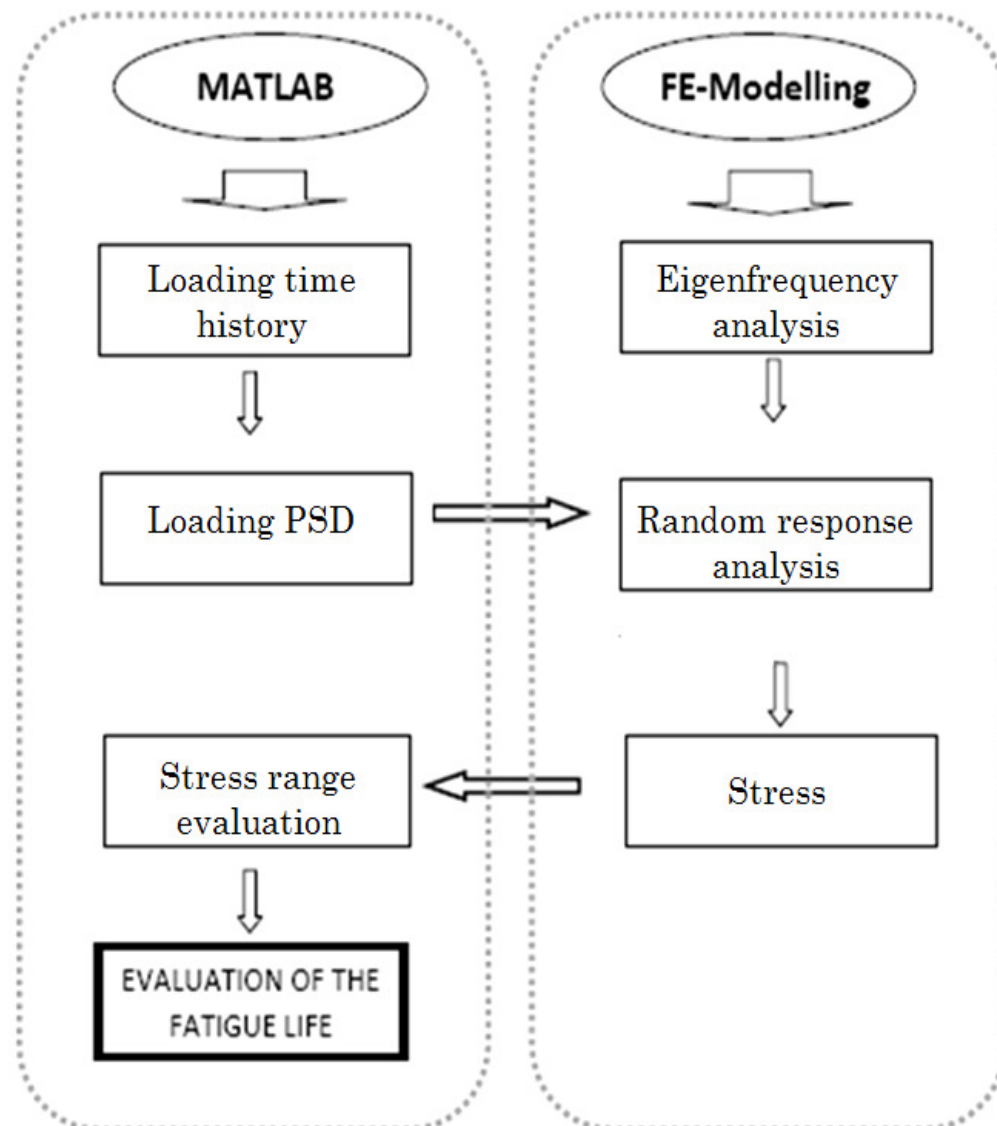


Figure (8-1) Flow chart of the process used for fatigue evaluation.

8.1 Response evaluation

A random response analysis was used to predict the response of the system subjected to a non-deterministic continuous excitation [19].

The response analysis is expressed as the power spectral density (PSD) of nodal variables, by using a path starting from the point where the stresses are the highest (the point where the stiffener is connected to the main web) as shown in Figure (8-2) and continuing in a vertical direction perpendicular to the weld toe.

The output PSD is obtained from the hot spot stress evaluation and has been done using the methodology described in Chapter 2.

The path is chosen where the largest deformation is found in the detail. Figure (7-8) indicates the deformation created by the applied load.

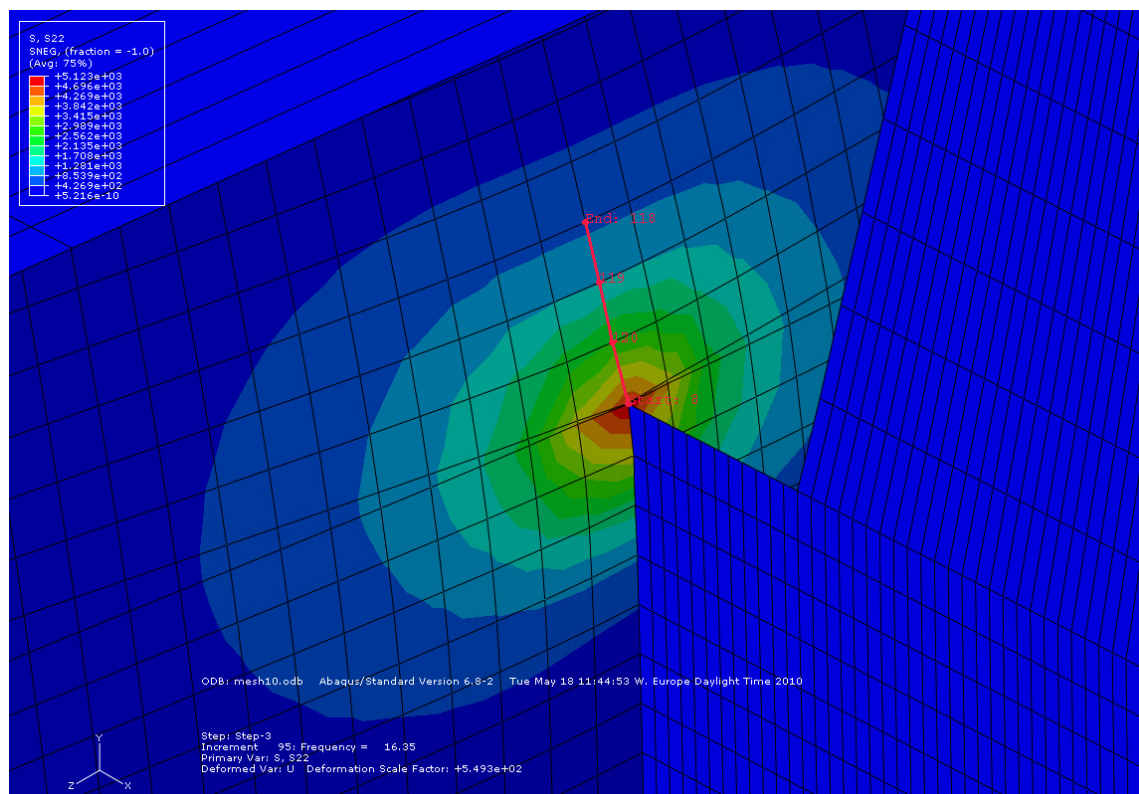


Figure (8-2) Path chosen in the detail to study the hot spot stresses

8.1.1 Output PSD from the averaged load

In order to calculate the hot spot stresses in the frequency domain, PSD of stress over the whole range of frequencies are calculated at different points along the path showed in Figure (8-2). These points are at the weld toe location and roughly 10, 20 and 30 mm from the weld toe. In Figure (8-3) the hot spot formulation, at the frequency of 16.35Hz can be observed. This formulation is repeated over the whole frequency spectrum to obtain the PSD of the hot spot stresses.

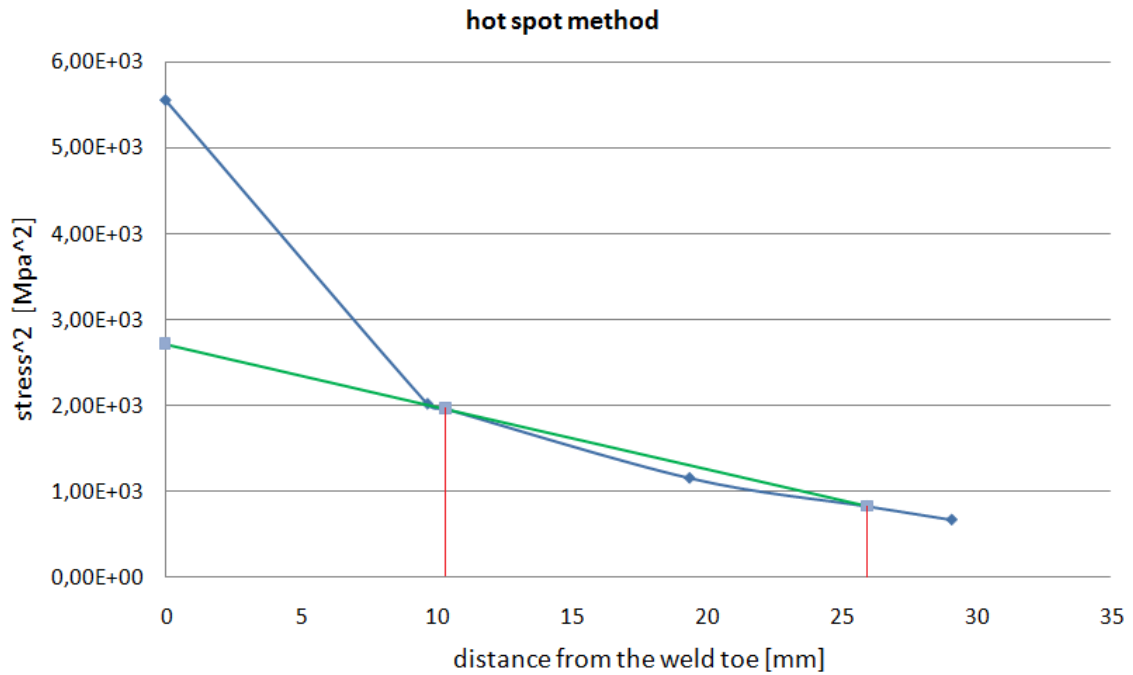


Figure (8-3) Hot spot formulation at the resonance frequency (16.35 Hz)

Furthermore, it is clearly noticed the big difference of the stresses between the hot spot stresses and the stresses at the weld toe. With the aim of calculating the fatigue life, only the hot spot stresses are used.

By analyzing the response function, Figure (8-4), it can be noticed that although the load is low at frequencies that are close to the detail resonance frequency, the response is large. This explains that the system behaves dynamically in terms of resonance, and emphasizes the importance to study fatigue by the dynamic approach. This peak at the resonance frequency could not have been captured with the traditional static approach.

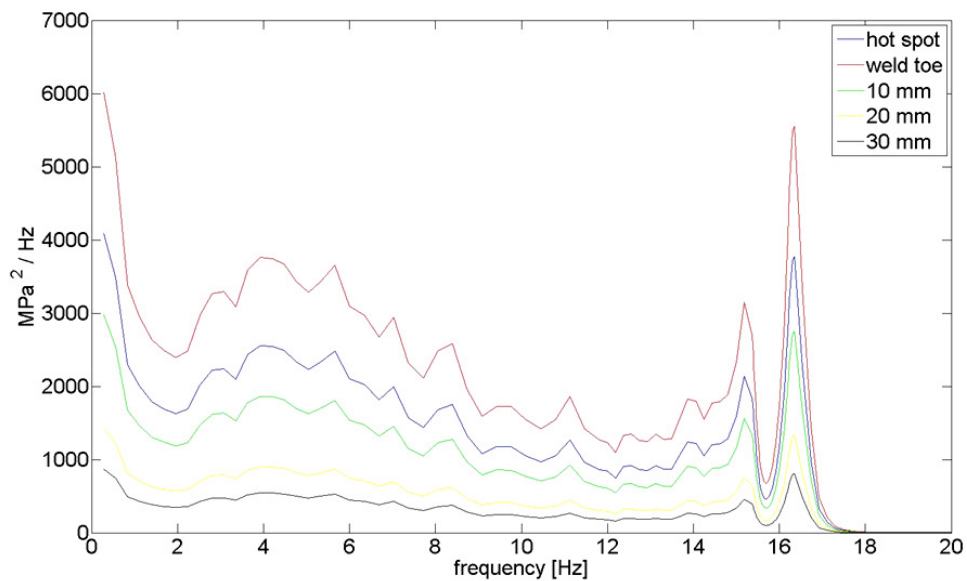


Figure (8-4) Hot spot method for the averaged load

By comparing the stress obtained at the lowest frequency in dynamic analysis with stress obtained for the static case applying the same load level; it can be observed that the system behaves quasi-static at low frequencies.

Table [8-1] Stresses at the static case and at low frequencies in the dynamic case [Mpa], both from the hot spot method

Stress at static case	53.0
Stress at the lowest frequency	67.4

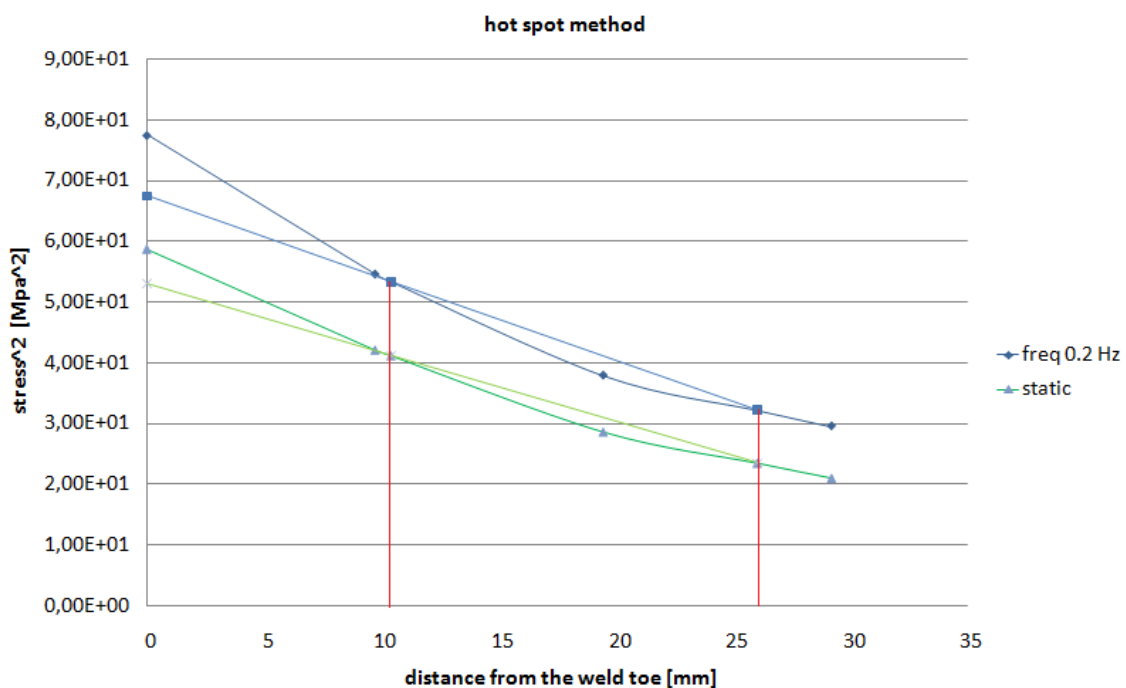


Figure (8-5) Comparison between hot spot stresses for static and dynamic loading conditions.

8.1.2 Output PSD from peak-hold load

Using the same procedure that has been outlined for the averaged load, the hot spot stresses have been calculated for the case of a peak-hold load spectrum. Figure (8-6) shows the peak-hold response. The shape of this response is similar to the averaged load. However the schema is higher simply because the input load has higher values at each frequency.

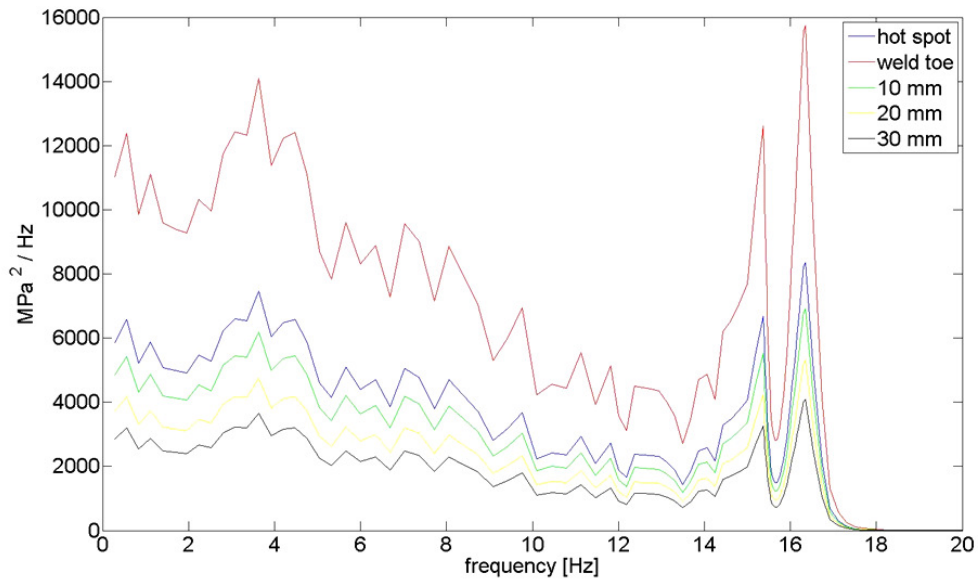


Figure (8-6) Hot spot response from peak-hold loading

8.1.3 Output PSD from the white noise load

The structural response due to White noise loading can be seen in Figure (8-7). The result indicates resonance frequencies clearly.

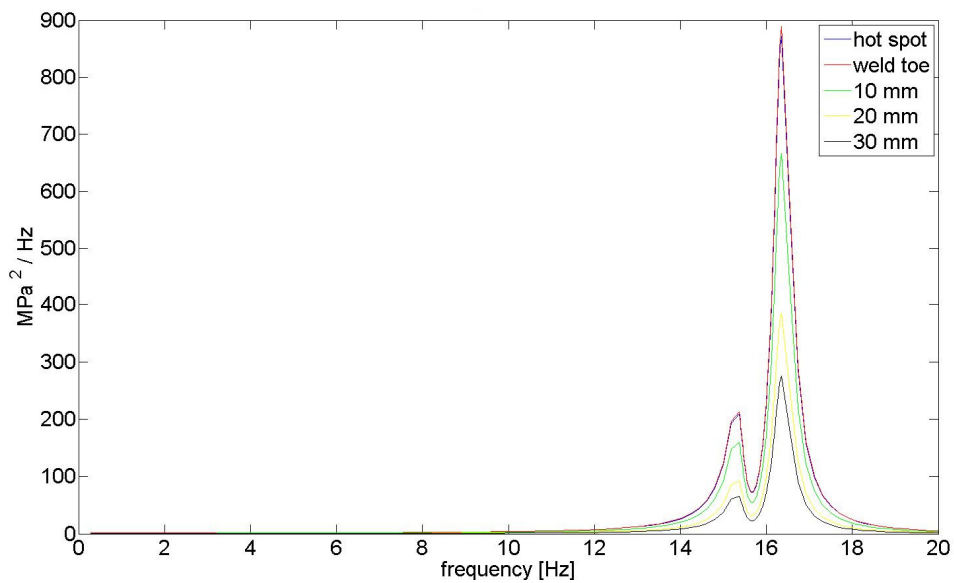


Figure (8-7) Hot spot response from white noise loading

8.2 Fatigue analysis

Once the stresses are obtained, they are evaluated in terms of probability density function before continuing estimating the fatigue life. Then, as explained in Chapter 6, an S-N curve of a specific detail category is used [4].

The structural detail of this study has the shape and loading as it is showed in the constructional detail number 5 from Table [2-1] where 100 is the detail category.

The algorithm for calculating the fatigue life from a stress pdf has been written in MATLAB software. To specify the detail category from the S-N curve the following algorithm has been used:

```
if stress(s)>74
    m=3;
else
    m=5;
end
C=5e6*74^m;
```

In Appendix B, fatigue damage is calculated by MATLAB software.

8.2.1 Fatigue estimation from the averaged load

By following the vibration fatigue approach in Equation (6-1), the fatigue damage will be determined. The probability density function of the stress range is obtained using Dirlik formula. In order to apply this method, the statistical properties of the time signal need to be determined by obtaining the moments of the response PSD. See Appendix B.

The probability density function of the stress range for the averaged load can be seen in Figure (8-8).

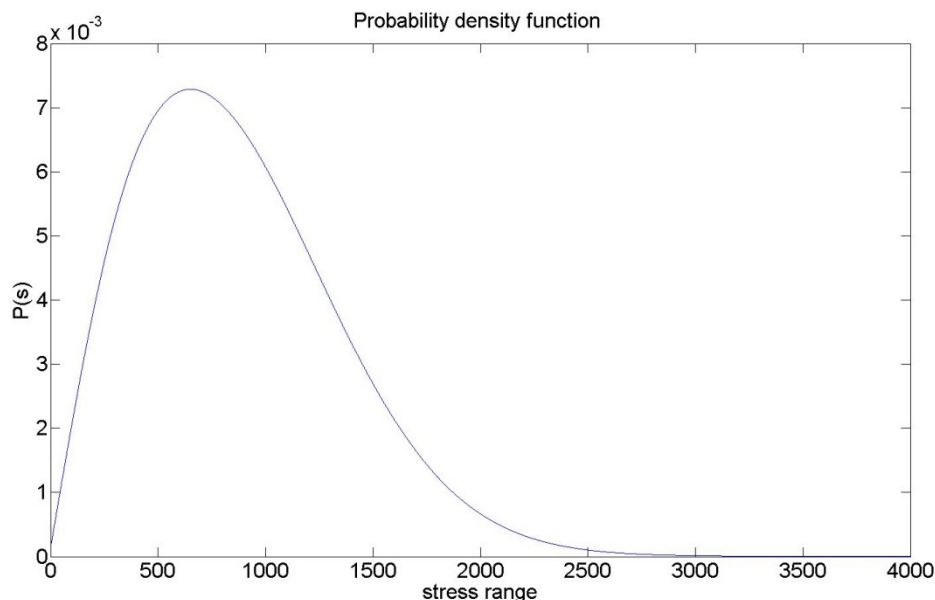


Figure (8-8) Probability density function (pdf)

Our structure is exposed to wide-band frequency excitation due to the train loads. The response of structures containing dynamic behavior at the resonance frequency is amplified when the frequency of the load is close to the resonance as it is showed in

Figure (8-4). Due to this phenomenon, it is observed how the fatigue life is considerably reduced at the resonance obtaining a fatigue life of 56 years. The fatigue life evaluated for the whole range of frequencies is showed in Figure (8-9).

For the frequencies that have no effect on the detail and do not cause any excitation for the structure, the fatigue life tends to be infinite and that is reasonable according to the fatigue definition.

It is interesting to see that in this case the fatigue failure is reached due to the static load, but it has almost the same fatigue life at the resonance frequency. Thus, this effect can only be captured using a dynamic approach.

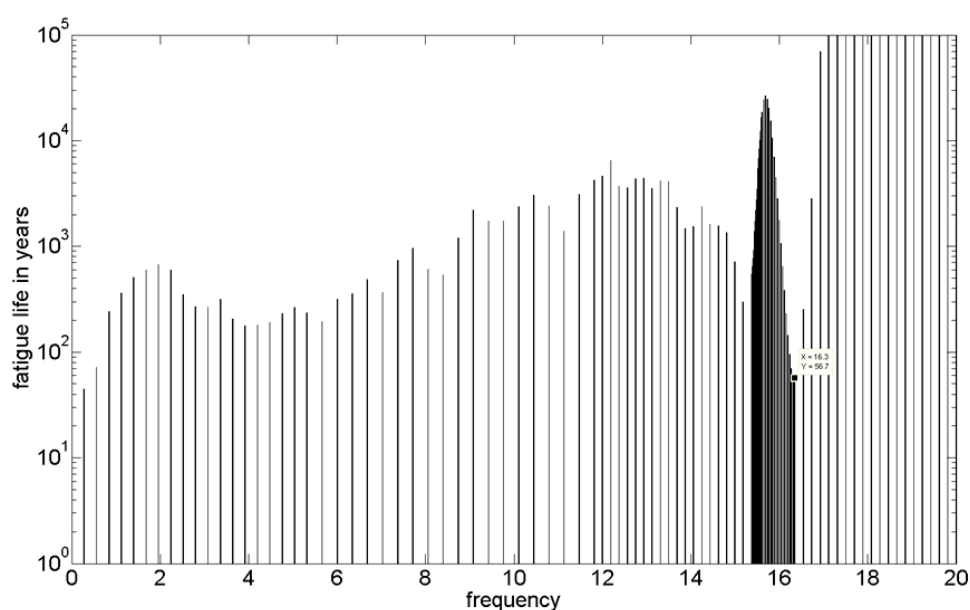


Figure (8-9) Fatigue life estimation for the averaged PSD method

The importance of using an adequate evaluation method of the stresses is demonstrated. In our work we could not performed a test base approach and compare the result with the FE analysis to verify this methodology. However it has been checked that the hot spot method gives accurate results when analyzing fatigue with FE analysis [6].

The difference in fatigue life by using both the hot spot method and no method can be clearly seen in Figure (8-10). Focusing at the resonance frequency of 16.3 Hz, a fatigue life of 19 years is obtained using no stress evaluation method, while using the hot spot method the fatigue life became 56 years.

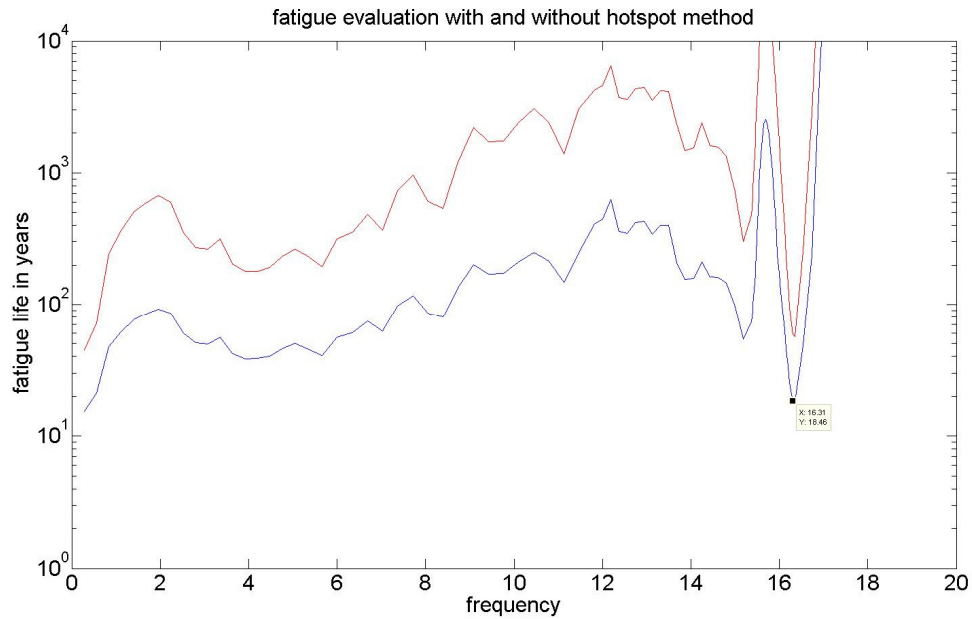


Figure (8-10) Comparison in fatigue life using hot spot method and no method for the averaged loading

8.2.2 Fatigue estimation from the peak-hold loading

Since the peak-hold loading is larger than the average loading, a higher fatigue damage estimation and thus the fatigue failure is produced for a life of 20 years at the resonance frequency which in comparison with the average method can be considered to be low. Fatigue life over the whole frequency spectrum can be observed in Figure (8-11).

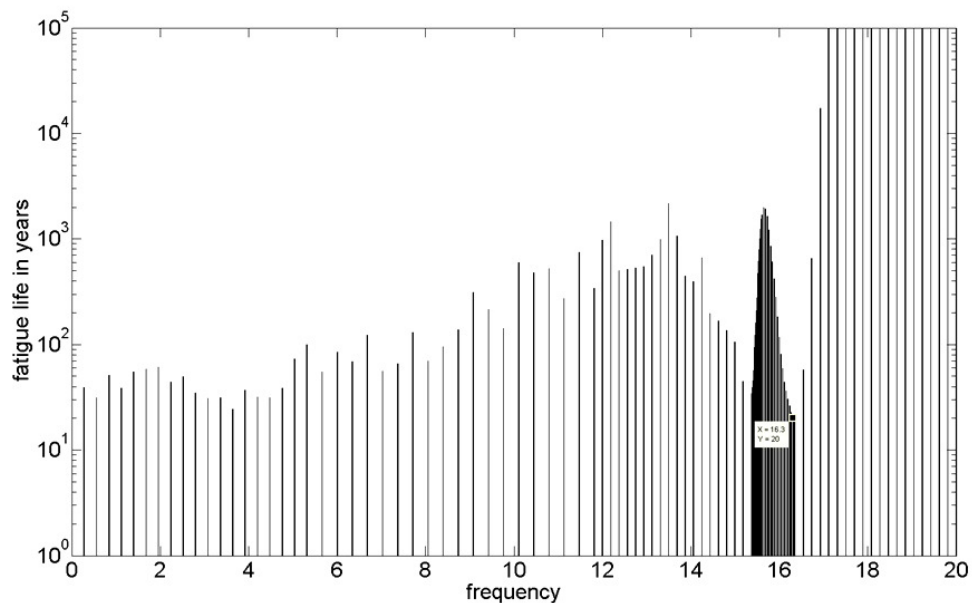


Figure (8-11) Fatigue life estimation for the peak-hold loading

8.2.3 Fatigue estimation from the white noise loading

By applying the white noise load and according to Figure (8-12), at the resonance frequency the fatigue life is about 70 years while at the rest of the frequencies it is infinite since the stress response out of the resonance frequency limits is almost zero.

The fatigue life obtained with this kind of load is not picked as relevant since the load level applied is too low. However, it is good to show the importance of a dynamic approach in structures with dynamic nature.

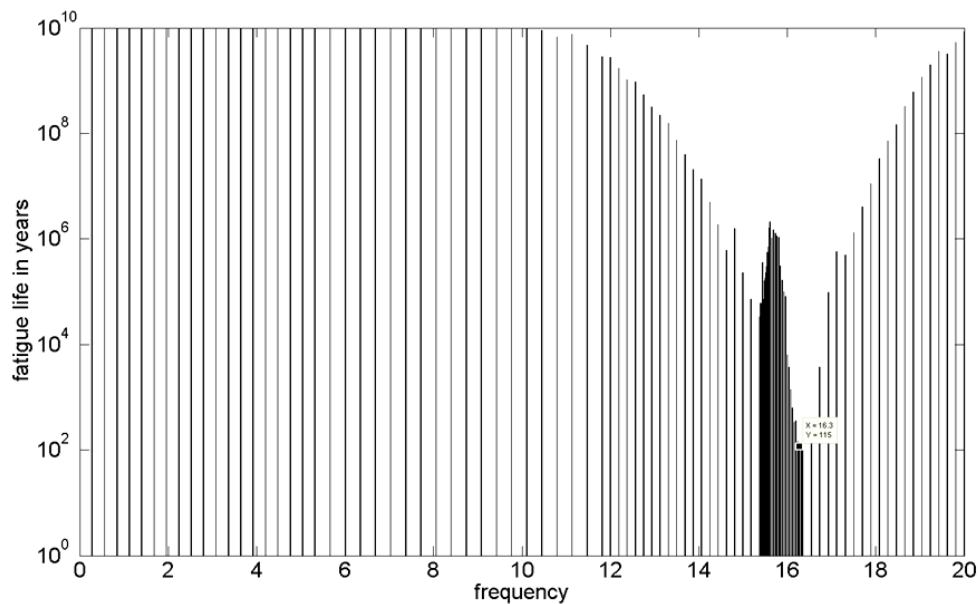


Figure (8-12) Fatigue life estimation for the white noise loading

8.2.4 Comparison of fatigue life between averaged, peak-hold and white noise loads

A comparison between the fatigue lives of the three different load spectrums: averaged, peak-hold and white noise, can be seen in Figure (8-13). As mentioned, the averaged load is picked to give the most reliable result, while the other two loads underestimate and overestimate the results respectively.

In this work the imperfections of the rail and the interaction between the wheels and the track are not considered. Furthermore, no impact loads are considered. In these cases, i.e. load with peaks, it could be necessary to study the peak-hold load spectrum that represents more accurately the loading case.

The White noise load is used to determine fatigue life of mechanical components that are exposed to vibrations in the whole frequency range. In this case, the load level of all the trains is low at high frequencies as it can be seen in Figure (4-8). However, the white noise load level remains constant in the whole frequency range, which not represents a train load.

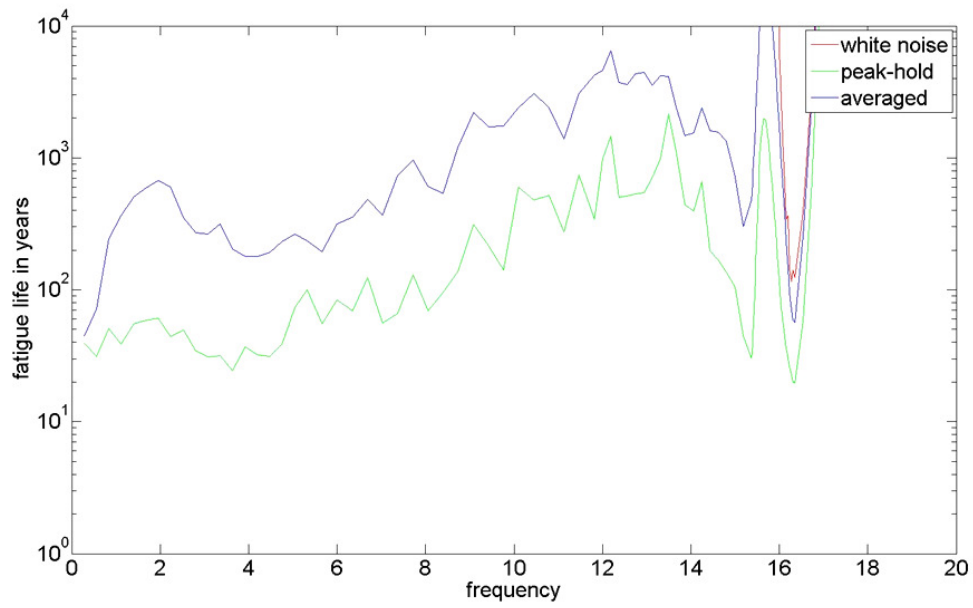


Figure (8-13) Comparison in fatigue lives

9 Conclusions

In accordance with the previous considerations, the results obtained were discussed and significant comparisons were made. The following conclusions can be drawn:

A dynamic approach may explain fatigue damage not captured using traditional methods. With the vibration fatigue analysis resonance phenomena due to dynamic loading is considered.

The structure behaved quasi static in terms of springiness and dynamically in terms of resonance.

A time domain approach requires an explicit load time history. To cover a wide range of loads, here trains and speeds, it may be more computationally efficient to use a frequency domain approach.

Mesh size in the Finite Element Modeling may influence the hot spot stresses. As the mesh become finer the stress goes higher. By performing a convergence study for the mesh, it is possible to assign the suitable mesh to determine the hot spot stresses.

The Narrow method for the pdf of rainflow ranges has been theoretically demonstrated to be a conservative solution. Many expressions have been proposed to correct the conservatism. However, Dirlik method is demonstrated to be the most accurate approach.

Different load cases are studied, however, note that neither the peak-hold method neither the white noise method accurately represents the actual vibration level of the bridge detail. The averaged load is picked to give the most reliable results.

10 Further studies

In this Master's thesis, the focus of study has been the usability of a frequency based approach to estimate the fatigue life of a structure subjected to dynamic loads.

An estimated fatigue damage based on Palmgren-Miner rule can be performed to compare the values obtained for both time and frequency domains.

A good way of comparing the result would be to use data measured on the actual bridge or to compare the result using an extensively advanced and already verified full bridge model.

The analysis is limited to a harmonic load that simulates trains moving at low speeds. The dynamic effects of the moving load must also be estimated in order to estimate impact the speeds of the trains have on the total dynamic response.

The interaction between train and rail had an effect on the dynamic response and need to be considered in order to perform a complete accurate dynamic analysis.

11 References

- 1- ESDEP, 1993. Extracts from the European Convention for Constructional Steelwork. Basic Introduction to fatigue, Chapter 12. Available at <http://www.esdep.org/members/master/toc.htm>
- 2- ESDEP. Extracts from the European Convention for Constructional Steelwork. Fatigue design concepts in Eurocode 3.
- 3- Al-Emrani, M. 'Fatigue in riveted railway bridges, a study of the fatigue performance of riveted stringers –to-floor-beam connections'' PhD thesis, Chalmers university, Göteborg, Sweden,2002
- 4- Eurocode 3: Design of steel structures- Part 1-9: 2005 *Fatigue*.
- 5- Niemi, E. & Marquis, G., 2002. Introduction to the structural stress approach to fatigue analysis of plate structures. *In processing of the IIW fatigue seminar*.
- 6- Eriksson, Å. et al., 2003. Weld evaluation using FEM: a guide to fatigue-loaded structures, Stockholm: Industrilitterature.
- 7- Radaj, D. & Cetin Morris. Fatigue assessment of welded joints by local approaches
- 8- Karlsson A. & Nilsson A. Dynamic analysis of railway bridges using the mode superposition method, *Master's Thesis in the International Master's programme Structural Engineering. Chalmers. Göteborg. Sweden 2007*
- 9- Bishop N. Vibration Fatigue Analysis in the Finite Element Environment, MSC Frimley and Alan Caserio, MSC Costa Mesa.
- 10- Bishop N., Lack L., Li T., Kent S. Analytical Fatigue life assessment of vibration induced fatigue damage. University College London
- 11- Kipp W. PSD and SRS in simple terms, Presented at ISTA Con '98, Orlando, Kipp Company LLC
- 12- Petrucci G. & Zuccarello B. On the estimation of the fatigue cycle distribution from spectral density data. Department of Mechanics and Aeronautics, University of Palermo, Italy.
- 13- Eurocode 3, EN 1991-2:2003(E)
- 14- Heiden M., Bokan H., Luís Simões da Silva, Greiner R., Pirchere M. & Pircher H. Dynamic effects of railway bridges for high speed.

- 15- Andersson A. Fatigue analysis of railway bridges- a full study of steel bridges between central Stockholm and Söder Mälärstrand, based on theoretical analysis and strain measurements. Swedish version, Stockholm 2009
- 16- Imam B., Righinioti T. & G. Kaliyaperumal. Advanced Dynamic Finite Element Analysis of a Skew Steel Railway Bridge.
- 17- Reinertsen 2004-02-12 besiktning rapport. Stoppborrning, lagerjustering samt besiktning av järnvägsbroar över Söderström och Söder Mälärstrand by. – Swedish version
- 18- Leander J. Rapport 126. Mätning och utvärdering m.a.p. utmattning, Trita-Bkn., Bygghvetenskap 2008
- 19- Fryba L. 1996. Dynamics of Railway Bridges. London : Thomas Telford,
- 20- ABAQUS, Inc., 2007. *ABAQUS analysis : User's manual 6.8*
- 21- Van Baren J. Vibration test replication of operating environment. *Vibration Research Corporation. Brian MacMillan.* Bruel & Kjaer UK Ltd., Stevenage, Hertfordshire , United Kingdom
- 22- Ragan P. & Manuel L., Civil, Architectural, and Environmental Engineering, University of Texas. *Comparing Estimates of Wind Turbine Fatigue Loads using Time- Domain and Spectral Methods.*
- 23- Kjell Eriksson, Fatigue, Att konstruera med stål, Läromedel för konstruktörer, Modul 8 utmattning, Luleå tekniska universitet, KTH Arkitektur och samhällsbyggnad, SBI- swedish version
- 24- Schijve J., Delft University of Technology, Netherland. *Fatigue of structures and materials.*
- 25- Akhlaghi F. Z. Fatigue life assessment of welded bridge detail using structural hot spot stress method- Master thesis 2009:104- Chalmers University of Technology. Göteborg, Sweden 2009.
- 26- Satish S. R. & Santha A.R., Indian Institute of Technology Madras. *Design of steel structures.* 1.7 Fatigue of steel structures.

- 27- P. D. Welch, "The use of fast Fourier transforms for the estimation of power spectra: A method based on time averaging over short modified periodograms," *IEEE Transactions on Audio and Electroacoustics*, vol. 15, pp. 70-73, 1967.
- 28- Roy R. Craig Jr., Andrew J. Kurdila. *Fundamentals of structural dynamics*. 2nd ed.
- 29- Paul A. Lynn, Wolfgang Fuerst. *Introductory Digital Signal Processing with Computer Applications*, 2nd Edition. Wiley.
- 30- X. Rong Li. *Probability, random signals and statistics*. CRC Press, 1999.
- 31- Daniel N. Rockmore. *The FFT – an algorithm the whole family can use*. Departments of mathematics and computer science, Dartmouth College, Hanover.
- 32- Bruno a. Olshausen. Aliasing. PSC 129 – Sensory Processes.
- 33- [33] Larsson. T., 2009. Fatigue assessment of riveted bridges. Luleå University of Technology. Department of Civil and Environmental Engineering. ISBN 978-91-86233-13-6

A.Appendix A

```

%-----
% DEFLECTION AT MID SPAN FOR VARIOUS VALUES OF SPEED
%-----
%% Introduction
%-----
% Program that calculates the deflection at mid span for a simply
support beam subjected to a moving load
%-----
%Clears all previous data
clear all
close all
clc
%%input data
A=0.335;
density=7850;
L= 33.675;           % length of the beam (m)
P=1;                % the load (N)
E=210e9;            %the modulus of elasticity (N/m^2)
J=0.637;            %the moment of inertia (m^4)
m=density*A;        % constant mass per unit length of the
                    % beam (Kg/m)
h=3.454;            % high of the beam IPE 600 (m)
v0=(P*(L^3))/(48*E*J) ; % The deflection at mid span of a beam
                    % loaded with static force (m)
M0=(P*L)/4;        % the bending moment at mid span of a
                    % beam loaded with static force [N*m]
w_e1= 0.003069;    % section modulus [m^3]
x=0.5*L;           %mid span length
c_cr=(pi/L)*sqrt(E*J/m); % the critical speed
psi=0.015;         %damping factor
length=2^10;       %number of samples

D=zeros(1,length);
T=zeros(1,length);
Strain=zeros(1,length);

z_c=0;
for c=1:25:101     % c=the constant speed at load motion
                    % (m/s)
    alpha=c/c_cr   % effect of speed
    w=pi*c/L;      % circular frequency
    t_f=L/c;       % final time
    dt=t_f/length; % time step
    z_c=z_c+1;
    i_t=0;
    for t=dt:dt:t_f
        v_f=0;
        M_f=0;
        i_t=i_t+1;

        for j=1:100

            w_j = sqrt(j^4*pi^4/L^4*E*J/m);
                    %circular frequency at the J-th mode of
                    % vibration
            w_1 = sqrt(1^4*pi^4/L^4*E*J/m);
            w_b =psi*w_1; %circular frequency of damping

```

```

wj=sqrt(w_j^2-w_b^2);
                                %Circular frequency of damping with
                                light damping
alpha = w/w_1;
beta = w_b/w_1;

v= v0 * ( ...
      (1/((j^2)*((j^2)*((j^2)-
              (alpha^2))^2+4*alpha^2*beta^2))) *
      ...
      ( j^2*(j^2-alpha^2)*sin(j*w*t) - ...
      ( ( j*alpha*(j^2*(j^2-alpha^2)-2*beta^2) ) /
              sqrt(j^4-beta^2) ) * ((exp(-w_b*t)) *
              sin(wj*t)) ) - ...
      ( 2*j*alpha*beta* ( cos(j*w*t) - (exp(-
              w_b*t))*cos(wj*t) ) ) ...
      )...
      ) ...
      * sin(j*pi*x/L);

v_0 = v + v_f;
v_f=v_0;

M = M0 * ((8*(j^2))/(pi^2))*sin((j*pi*x)/L) * ( ...
      (1/((j^2)*((j^2)*((j^2)-
              (alpha^2))^2+4*alpha^2*beta^2))) *
      ...
      ( j^2*(j^2-alpha^2)*sin(j*w*t) - ...
      ( ( j*alpha*(j^2*(j^2-alpha^2)-2*beta^2) ) /
              sqrt(j^4-beta^2) ) * ((exp(-w_b*t)) *
              sin(wj*t)) ) - ...
      ( 2*j*alpha*beta* ( cos(j*w*t) - (exp(-
              w_b*t))*cos(wj*t) ) ) ...
      )...
      ) ;
M_0 = M + M_f;
M_f=M_0;

end

D(1,i_t)=v_f;
X=(L/length)*(1:length);
end

Df(z_c,:)=D(1,:);

end
figure
plot(X/L,-Df,'-',X/L,-v0,'--');
title('Deflection at mid span for various values of
      speed','FontSize', 24)
xlabel(' load position X/L','FontSize', 24)
ylabel('deflection at x=L/2','FontSize', 24)

```


B. Appendix B

```

%-----
% FATIGUE ANALYSIS
%-----
%% Introduction
%-----
% Program that calculates:
%   -Train load based on HSLM-A
%   -Hot spot stresses
%   -PSD moments
%   -Probability density function of stress range
%   -Fatigue life by vibration fatigue approach
%-----
%Clears all previous data
clear all;
close all;
clc;
set(0,'defaultAxesFontSize',24)

d=1000*[2 3.5 2 3 2 2 2 2.5 2 2];
D=1000*[18 19 20 21 22 23 24 25 26 27];
N=[18 17 16 15 14 13 13 12 11 11];
P=1000*[170 200 180 190 170 180 190 190 210 210];

count_c=0;
v_min=(10*10000/36);
v_max=(50*10000/36);

for i=1:10;

    L=N(i)*D(i);

    for c=v_min: (5*10000/36): v_max;
        count_c=count_c+1;
        t_f=((3000.525-d(i)/2)*2+41000.05-
            d(i)+(N(i)+2)*D(i)+3)/(10*10000/36);
        NFFT=2^14;
        Fs=NFFT/t_f; %samples/unit time
        t = 1/Fs : 1/Fs: t_f; %time range

        d1 = (3000.525-d(i)/2+20000.525)/c : D(i)/c : (3000.525-
            d(i)/2+20000.525+(N(i)+1)*D(i)+D/2)/c;
        f1=1/(D(i)/c);

        d2 = (3000.525-d(i)/2+20000.525+d(i))/c : (D(i)-
            2*d(i)+N(i)*D(i)+D(i)-d(i))/c :
            (41000.05-d(i)+(N(i)+2)*D(i))/c;
        f2=1/((D(i)-2*d(i)+N(i)*D(i)+D(i)-d(i))/c);

        d3 = (3000.525-d(i)/2+20000.525+D(i)-d(i))/c : D(i)/c :
            (3000.525-d(i)/2+20000.525+D(i)-
            d(i)+(N(i)+1)*D(i)+D(i)/2)/c;

        d4 = (3000.525-d(i)/2)/c : (24000.05-d(i)+(N(i)+2)*D(i))/c :
            (41000.05-d(i)+(N(i)+2)*D(i))/c;
        f4=1/((24000.05-d(i)+(N(i)+2)*D(i))/c);
    end
end

```

```

d5 = (3000.525-d(i)/2+3000)/c : (24000.05-d(i)+(N(i)+2)*D(i))/c
      : (41000.05-d(i)+(N(i)+2)*D(i))/c;

d6 = (3000.525-d(i)/2+14000)/c : (24000.05-
      d(i)+(N(i)+2)*D(i))/c : (41000.05-
      d(i)+(N(i)+2)*D(i))/c;

d7 = (3000.525-d(i)/2+17000)/c : (24000.05-
      d(i)+(N(i)+2)*D(i))/c : (41000.05-
      d(i)+(N(i)+2)*D(i)+3)/c;

y1 = pulstran(t,d1,'tripuls',0.1,0);
y2 = pulstran(t,d2,'tripuls',0.1,0);
y3 = pulstran(t,d3,'tripuls',0.1,0);
y4 = pulstran(t,d4,'tripuls',0.1,0);
y5 = pulstran(t,d5,'tripuls',0.1,0);
y6 = pulstran(t,d6,'tripuls',0.1,0);
y7 = pulstran(t,d7,'tripuls',0.1,0);

y = (P(i)*(y1+y2+y3+y4+y5+y6+y7));

NFFT2=NFFT/2^5;
window=hanning(NFFT2);
[psd(count_c,:),f(count_c,)] = pwelch(y,window,0.05,NFFT2,Fs);

end

end
f2=f(1,:);
psd2=mean(psd,1)/max(mean(psd,1));
for x=1:length(f2)
    PSD(x,1)=psd2(x);
    PSD(x,2)=0;
    PSD(x,3)=f2(x);
end

figure
plot(f(1,:),psd2);
title('input psd ','FontSize', 24)
xlabel('Frequency (Hz)','FontSize', 24);
ylabel('S_F (N^2/Hz)','FontSize', 24);
axis([0 20 0 1])

save PSD_averaged.txt PSD -ASCII
%-----
%% Calculate Hot spot stresses
%-----

load hot_spot0.txt
load hot_spot_10.txt
load hot_spot_20.txt
load hot_spot_30.txt

f_hs=hot_spot0(:,1)';
s_0=hot_spot0(:,2);
s_10=hot_spot_10(:,2);
s_20=hot_spot_20(:,2);
s_30=hot_spot_30(:,2);

```

```

length_s=length(s_0);

for s=1:length_s;
    sigma_10_4(s)=s_20(s)-((s_20(s)-s_10(s))/(19.4-9.7))*(19.4-10.4);
    sigma_26(s)=s_30(s)-((s_30(s)-s_20(s))/(29.1-19.4))*(29.1-26);

    sigma_hs(s)=1.67*sigma_10_4(s)-0.67*sigma_26(s);
end

figure
plot(f_hs,sigma_hs,'b',f_hs,s_0,'r',f_hs,s_10,'g',f_hs,s_20,'y',f_hs,s_
      30,'k')
title('hot spot method ','FontSize', 24)
xlabel('frequency [Hz]','FontSize', 24)
ylabel('MPa ^2 / Hz','FontSize', 24)

sigma=sigma_hs/max(sigma_hs);
figure
plot(f_hs,sigma,'b')
title('hot spot stress ','FontSize', 24)
xlabel('frequency [Hz]','FontSize', 24)
ylabel('S_s_i_g_m_a [MPa ^2 / Hz]','FontSize', 24)

%-----
%% Calculate PSD moments
%-----
f1=f_hs;
PSD=sigma_hs;
p=length(PSD);
for i=1:p
    if i==p
        i=p-1;
        df(p)=(f1(i+1)+f1(i))/2-(f1(i-1)+f1(i))/2;
    end
    if i==1
        i=2;
        df(1)=(f1(i+1)+f1(i))/2-(f1(i-1)+f1(i))/2;
    end
    df(i)=(f1(i+1)+f1(i))/2-(f1(i-1)+f1(i))/2;
end
m0=0;
for i=1:p
    m0=m0+PSD(1,i)*df(i);
end;

m1=0;
for i=1:p
    m1=m1+f1(1,i)*PSD(1,i)*df(i);
end;

m2=0;
for i=1:p
    m2=m2+f1(1,i)^2*PSD(1,i)*df(i);
end;

m4=0;
for i=1:p
    m4=m4+(f1(1,i)^4)*PSD(1,i)*df(i);
end;
m0
rms=sqrt(m0)

```

```

m1
m2
m4

E_0=sqrt(m2/m0)
E_p=sqrt(m4/m2)
gamma=E_0/E_p

%-----
%% Calculate the probability density function of stress range using
%% Dirlik method
%-----
stress=sqrt(sigma_hs);           %range stress value
f_s=f_hs;

Ls=length(stress);
ds=(max(stress)-min(stress))/Ls;
stress_2=ds:ds:4000;
L1=length(stress_2);

for s=1:L1;
    z(s)=stress_2(s)/(2*sqrt(m0));
    X_m=(m1/m0)*sqrt(m2/m4);
    D1=(2*(X_m-gamma^2))/(1+gamma^2);
    R=(gamma-X_m-D1^2)/(1-gamma-D1+D1^2);
    D2=(1-gamma-D1+D1^2)/(1-R);
    Q=(5*(gamma-D1-D2*R))/(4*D1);
    D3=1-D1-D2;

    P(s)=(D1/Q)*exp(-z(s)/Q)+(D2*z(s)/R^2)*exp((-
                                                z(s)^2)/2*R^2)+D3*z(s)*exp(-
                                                z(s)^2/2))/(2*sqrt(m0));

end

figure
plot(stress_2,P)
title('Probability density function ','FontSize', 24)
xlabel('stress range','FontSize', 24)
ylabel('P(s)','FontSize', 24)

%-----
%% Calculate fatigue life from a stress PDF
%-----

Total_damage=0;
L2=length(stress);
stress_s=sort(stress);
for s=1:L2;

    T=1;
    if stress(s)>74
        m=3;
    else
        m=5;
    end
    C=5e6*74^m;

    z(s)=stress(s)/(2*sqrt(m0));
    X_m=(m1/m0)*sqrt(m2/m4);
    D1=(2*(X_m-gamma^2))/(1+gamma^2);

```

```

R=(gamma-X_m-D1^2)/(1-gamma-D1+D1^2);
D2=(1-gamma-D1+D1^2)/(1-R);
Q=(5*(gamma-D1-D2*R))/(4*D1);
D3=1-D1-D2;

P(s)=(D1/Q)*exp(-z(s)/Q)+(D2*z(s)/R^2)*exp((-
        z(s)^2/2*R^2)+D3*z(s)*exp(-
        z(s)^2/2))/(2*sqrt(m0));
ff=find(stress_s==stress(s));
    if ff==L2
        ff=L2-1;
    end
    if ff==1
        ff=2;
    end

    dS(s)=(stress_s(ff+1)+stress_s(ff))/2-(stress_s(ff-
        1)+stress_s(ff))/2;

    E_D(s) = E_p*T/C*(stress(s)^m*P(s)* dS(s));
    fatigue_life(s)=(1/E_D(s))/(3600*24*365);
    Total_damage=Total_damage+E_D(s);
end

Total_damage

figure
bar(f_s,E_D)
ax = axis;
set(gca,'yscale','log')
axis(ax)
ylabel('damage per second','FontSize',24)
xlabel('frequency','FontSize',24)

figure
bar(f_s,fatigue_life)
ax = axis;
set(gca,'yscale','log')
axis(ax)
ylabel('fatigue life in years','FontSize',24)
xlabel('frequency','FontSize',24)
axis([0 20 0 1e5])

```

C.Appendix C

In this appendix, the “input file” used to calculate the random response in Abaqus is presented. This is not the complete file, node and element numbers are removed because they are not relevant to understand the code.

```
** -----
*Heading
** Job name: random_response Model name: Model-1
** Generated by: Abaqus Version 6.8-2
** Preprint, echo=NO, model=NO, history=NO, contact=NO
** -----
** PARTS
**
*Part, name=Part-1
*End Part
**
*Part, name=connector1
*End Part
**
*Part, name=connector2
*End Part
** -----
** ASSEMBLY
**
*Assembly, name=Assembly
**
*Instance, name=Part-1-1, part=Part-1
*Node
    1,          1260.,          2948.,          3368.
    2,          1260.,          2698.,          3368.

    25601,      6036.92285,          1068.,          3347.83984
    25602,      6198.46143,          1068.,          3347.60742
**
*Element, type=S4R
    1,    1,    97, 2804, 130

25245,    957,    48, 2803, 25602
**
** Section: shell_26
*Shell Section, elset=_PickedSet2_#1, material=steel
26., 5
** Section: shell_52
*Shell Section, elset=_PickedSet3_#1, material=steel
52., 5
** Section: shell_50
*Shell Section, elset=_PickedSet2_#4, material=steel
50., 5
** Section: shell_52
*Shell Section, elset=_PickedSet3_#2, material=steel
52., 5
** Section: shell_16
*Shell Section, elset=_PickedSet2_#2, material=steel
16., 5
** Section: shell_15
*Shell Section, elset=_PickedSet3_#15, material=steel
15., 5
** Section: shell_50
*Shell Section, elset=_PickedSet4_#15, material=steel
50., 5
*End Instance
**
*Instance, name=connector1-1, part=connector1
    1560.,          2913.,          3343.

90.
*Node
    1,          0.,          35.,          0.

    210,          50.,          0.,          200.
```

```

*Element, type=C3D8R
  1, 71, 72, 86, 85, 1, 2, 16, 15

104, 195, 196, 210, 209, 125, 126, 140, 139
*Nset, nset=_PickedSet2, internal, generate
  1, 210, 1
*Elset, elset=_PickedSet2, internal, generate
  1, 104, 1
** Section: solid
*Solid Section, elset=_PickedSet2, material=steel

*End Instance
**
*Instance, name=connector2-1, part=connector2
  1180., 2913., 3343.
  1180., 2913., 3343., 1180., 2912., 3343.,
  90.
*Node
  1, 0., 35., 0.
  2200, 50., 0., 120.
*Element, type=C3D8R
  1, 276, 277, 302, 301, 1, 2, 27, 26

1680, 2174, 2175, 2200, 2199, 1899, 1900, 1925, 1924
** -----
** MATERIALS
**
*Material, name=steel
*Damping, composite=0.015
*Density
  7.85e-09,
*Elastic
210000., 0.27
** -----
** INTERACTION PROPERTIES
**
*Surface Interaction, name=IntProp-1
1.,
*Friction
0.,
*Surface Behavior, penalty
*Surface Interaction, name=IntProp-2
1.,
*Friction
0.,
** -----
** INTERACTIONS
**
** Interaction: Int-1
*Contact Pair, interaction=IntProp-1, type=SURFACE TO SURFACE, no thickness, adjust=50.
_PickedSurf726, Surf-connector1
** Interaction: Int-2
*Contact Pair, interaction=IntProp-2, type=SURFACE TO SURFACE, no thickness, adjust=50.
_PickedSurf727, Surf-connector2
** Interaction: Int-3
*Contact Pair, interaction=IntProp-1, adjust=Set-7
_PickedSet636_CNS_, _PickedSurf635
** Interaction: Int-4
*Contact Pair, interaction=IntProp-2, small sliding, type=SURFACE TO SURFACE, no
thickness, adjust=Set-8
_PickedSurf639, _PickedSurf638
** -----
**PSD
**
*PSD-DEFINITION, NAME=PSD, TYPE=FORCE, INPUT=PSD.txt
** -----
** STEP: Step-1
**
*Step, name=Step-1
*Static
1., 1., 1e-05, 1.
** BOUNDARY CONDITIONS
**
** Name: BC-1 Type: Displacement/Rotation
*Boundary
_PickedSet744, 1, 1

```

```

_PickedSet744, 2, 2
_PickedSet744, 3, 3
** Name: BC-2 Type: Displacement/Rotation
*Boundary
_PickedSet743, 1, 1
_PickedSet743, 2, 2
_PickedSet743, 3, 3
** INTERACTIONS
**
** Contact Controls for Interaction: Int-1
*Contact Controls, master=Surf-connector1, slave=_PickedSurf726, reset
*Contact Controls, master=Surf-connector1, slave=_PickedSurf726, automaticTolerances,
stabilize=1.
** Contact Controls for Interaction: Int-2
*Contact Controls, master=Surf-connector2, slave=_PickedSurf727, reset
*Contact Controls, master=Surf-connector2, slave=_PickedSurf727, automaticTolerances,
stabilize=1.
** OUTPUT REQUESTS
**
*Restart, write, frequency=0
**
** FIELD OUTPUT: F-Output-1
**
*Output, field, variable=PRESELECT
**
** HISTORY OUTPUT: H-Output-1
**
*Output, history, variable=PRESELECT
*End Step
** -----
** STEP: Step-2
**
*Step, name=Step-2, perturbation
*Frequency, eigensolver=Lanczos, acoustic coupling=off, normalization=displacement,
number interval=1, bias=1.
, , 50. , ,
**
** OUTPUT REQUESTS
**
*Restart, write, frequency=0
**
** FIELD OUTPUT: F-Output-2
**
*Output, field, variable=PRESELECT
*End Step
** -----
** STEP: Step-3
**
*Step, name=Step-3, perturbation
*Random Response
0, 20, 20, 1, 1
*Modal Damping, modal=COMPOSITE
1, 15
** LOADS
**
** Name: Load-1 Type: Concentrated force
*Cload, load case=1
_PickedSet605, 2, -1
*CORRELATION, TYPE=CORRELATED, PSD
1,1,0
**
** OUTPUT REQUESTS
**
** FIELD OUTPUT: F-Output-3
**
*Output, field, variable=PRESELECT
*Output, history, frequency=0
*End Step

```